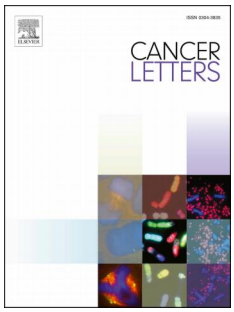

Arctigenin disrupts NLRP3 inflammasome assembly in colonic macrophages *via* downregulating fatty acid oxidation to prevent colitis-associated cancer

Simiao Qiao, Changjun Lv, Yu Tao, Yumeng Miao, Yanrong Zhu, Wenjie Zhang, Dandan Sun, Xinming Yun, Yufeng Xia, Zhifeng Wei, Yue Dai

PII: S0304-3835(20)30447-X

DOI: https://doi.org/10.1016/j.canlet.2020.08.033

Reference: CAN 114922

To appear in: *Cancer Letters*

Received Date: 18 June 2020

Revised Date: 9 August 2020

Accepted Date: 23 August 2020

Please cite this article as: S. Qiao, C. Lv, Y. Tao, Y. Miao, Y. Zhu, W. Zhang, D. Sun, X. Yun, Y. Xia, Z. Wei, Y. Dai, Arctigenin disrupts NLRP3 inflammasome assembly in colonic macrophages *via* downregulating fatty acid oxidation to prevent colitis-associated cancer, *Cancer Letters* (2020), doi: https://doi.org/10.1016/j.canlet.2020.08.033.

CRediT author statement

Qiao Simiao: Conceptualization, Methodology, Validation, Formal analysis, Writing-Original draft preparation. **Lv Changjun**: Methodology, Validation. **Tao Yu**: Formal analysis. **Miao Yumeng**: Methodology, Resources. **Zhu Yanrong, Zhang Wenjie and Sun Dandan**: Methodology. **Yun Xinming**: Methodology, Validation. **Xia Yufeng**: Project administration, Funding acquisition. **Wei Zhifeng**: Writing-Reviewing and Editing. **Dai Yue:** Conceptualization, Writing- Reviewing and Editing, Project administration, Funding acquisition, Supervision.

Title：

Arctigenin disrupts NLRP3 inflammasome assembly in colonic macrophages *via* downregulating fatty acid oxidation to prevent colitis-associated cancer

Simiao Qiao, Changjun Lv, Yu Tao, Yumeng Miao, Yanrong Zhu, Wenjie Zhang, Dandan Sun, Xinming Yun, Yufeng Xia, Zhifeng Wei*, Yue Dai*

Department of Pharmacology of Chinese Materia Medica, School of Traditional Chinese Pharmacy, China Pharmaceutical University, 24 Tong Jia Xiang, Nanjing 210009, China

*Corresponding author: Department of Pharmacology of Chinese Materia Medica, China Pharmaceutical University, 24 Tong Jia Xiang, Nanjing 210009, China. Tel.: +86 25 83271400; Fax: +86 25 85301528.

E-mail: yuedaicpu@cpu.edu.cn (Yue Dai); 1020132346@cpu.edu.cn (Zhifeng Wei)

Abstract

Arctigenin, the major active constituent of Fructus Arctii, has been reported to inhibit the growth of various tumors and alleviate colitis. This study aimed to prove the protective effect of arctigenin on colitis-associated cancer (CAC) and explore its mechanisms. Orally administered arctigenin prevented the progression of colitis and protected against colon carcinogenesis in azoxymethane (AOM)/dextran sulfate sodium (DSS)-induced CAC mice. Arctigenin downregulated NLRP3 inflammasome activation and fatty acid oxidation (FAO) metabolism in macrophages, as determined by untargeted metabolomics. Arctigenin also inhibited the expression of carnitine palmitoyltransferase 1 (CPT1), reduced the acetylation of α-tubulin, and disrupted NLRP3 complex formation, which in turn inactivated the NLRP3 inflammasome. Downregulation of the CPT1-FAO-acetyl-coenzyme A (acetyl-CoA)-acetylated α-tubulin pathway was observed to inhibit the effect of arctigenin on NLRP3 inflammasome assembly, as confirmed by CPT1 overexpression. Lastly, arctigenin was shown to inhibit NLRP3 inflammasome activation and improve CAC in mice, and the effect was significantly diminished by the overexpression of adeno-associated virus (AAV)9-CPT1. Taken together, these results show that the inhibition of NLRP3 inflammasome assembly in macrophages due to FAO downregulation contributes to the preventative effect of arctigenin against CAC. Our findings highlight the potential value of arctigenin to reduce the risk of CAC in patients with colitis.

Keywords: arctigenin; colitis-associated cancer; NLRP3 inflammasome; fatty acid oxidation; carnitine palmitoyltransferase 1

Graphical abstract

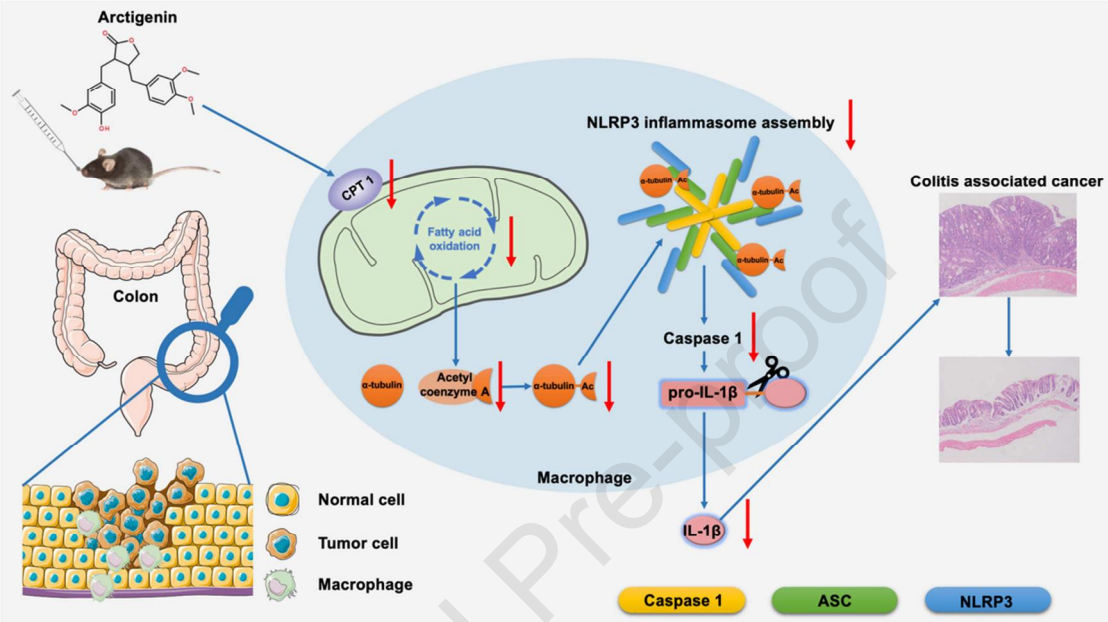

1. Introduction

Colorectal cancer (CRC) ranks third among all types of cancer in terms of incidence and second in terms of mortality. In 2018, an estimated 1.8 million new CRC cases were diagnosed[1, 2]. The pathophysiological properties of CRC have yet to be fully explored. The epidemiological and experimental literature suggests that chronic inflammation is a primary risk factor for the development of CRC. Patients with ulcerative colitis, a common inflammatory bowel disease (IBD), are up to 30 times more likely to develop CRC comparing to healthy individual[3, 4]. Colitis-associated cancer (CAC) is an important subtype of CRC[5]. CRC patients lack symptomatic clinical features in the early stage, which makes clinical diagnosis difficult while the disease is still curable challenging[6]. Preventive strategies, including the control of IBD, are undoubtedly valuable for the management of CRC.

Although the precise pathogenesis of the development of chronic colitis to carcinogenesis has yet to be identified, a portfolio of cytokines including tumor necrosis factor-α (TNF-α), interleukin-1β (IL-1β), and IL-6, which are mainly secreted by macrophages in the inflammatory milieu of the colon, has been shown to play key roles in this process[7]. Zaki et al. observed elevated levels of these cytokines in the blood and colonic mucosa of IBD patients and CAC model mice[8]. TNF-α can stimulate the production of the molecules that cause DNA damage and mutations. IL-6 can promote the survival of the neoplastic colon epithelial cells during the

development of CAC. More importantly, IL-1β participates in the differentiation, proliferation, and activation of immune cells, and eventually facilitates the perpetuation of colitis and the progression of CAC[9]. The inflammasome is a multiprotein complex that is well known to be critical for the production of IL-1β. One of the most intensively studied inflammasomes is the NACHT, LRR, and PYD domain-containing protein 3 (NLRP3) inflammasome, which contains the sensor NLRP3, an apoptosis-associated speck-like protein containing a CARD (ASC) adaptor and caspase-1 protease[10]. Early studies demonstrated that mice with NLRP3, ASC, or IL-1β deficiency were protected from experimental colitis and the induction and progression of CRC[11]. Furthermore, in NLRP3- and caspase-1-deficient mice, the proliferation of gastrointestinal epithelial cells was found to be reduced[12].

Further studies have demonstrated that the distinct commensal bacterial species *Proteus mirabilis* can induce robust secretion of IL-1β via activation of the NLRP3 inflammasome in intestinal $Ly6C^{high}$ monocytes in dextran sulfate sodium (DSS)-induced colitis, which could be linked to the increased severity of colitis[13]. The over-activation of the NLRP3 inflammasome and subsequent excess secretion of mature IL-1β can mediate tissue damage and promote intestinal inflammation[14]. Therefore, the prevention of excessive activation of the NLRP3 inflammasome can be beneficial for hindering the development of CAC.

Arctigenin is a lignin ingredient isolated from the dried fruits of *Arctium lappa* L. (Fructus Arctii), a herbal medicine commonly used in China and Japan. Our previous studies demonstrated that orally administered arctigenin substantially ameliorated DSS-induced colitis in mice by inhibiting Th1 and Th17 cell responses[15]. Other research groups have reported that arctigenin exerted prominent anti-tumor activities *in vivo* and *vitro*[16-18]. In particular, a multicenter phase II clinical trial (UMIN000010111) is underway to evaluate the efficacy and safety of arctigenin in the treatment of pancreatic cancer patients who are refractory to gemcitabine and fluoropyrimidine [19,20]. These findings suggest that arctigenin has therapeutic potential against CRC. In the present study, we studied the effects of arctigenin on azoxymethane (AOM)/DSS-induced CAC in mice and the underlying mechanisms based on the activation of the NLRP3 inflammasome in colonic macrophages.

2. Materials and methods

2.1 Materials

Arctigenin (purity > 98 %) was purchased from Xi'an Ciyuan Pharmaceutical Co. Ltd. Mesalazine was obtained from Ethypharm Pharmaceutical Co Ltd. AOM, lipopolysaccharide (LPS, E. coli: Serotype O55:B5), etomoxir (ETX), and dimethyl sulfoxide (DMSO) were purchased from Sigma-Aldrich (St. Louis, USA). DSS (molecular weight: 36000–50000 Da) was supplied by MP Biomedical (Irvine, USA). Enzyme-linked immunosorbent assay (ELISA) kits (TNF-α, IL-1β, IL-6, and IL-17) were obtained from Dakewe Biotech (Shenzhen, China), ELISA kits for acetyl coenzyme A (acetyl-CoA) were obtained from BioVision (San Francisco, USA), and ELISA kits for IL-18 were obtained from Lianke Biotech (Hangzhou, China). TRIzol reagent was purchased from Invitrogen (CA, USA). RIPA buffer, NP-40 buffer, bovine serum albumin (BSA), and 2-(4-amidinophenyl)-6-indolecarbamidine dihydrochloride (DAPI) were purchased from Beyotime Biotechnology (Shanghai, China). Protease inhibitor cocktail was purchased from Boster Biological Technology Co. Ltd (Wuhan China); Primary antibodies against NLRP3 (15101S), pro-IL-1β (12242S), and IL-1β (52718S and 83186S) were obtained from Cell Signaling Technology (MA, USA), primary antibody against ASC (sc-514414) was purchased from Santa Cruz (CA, USA), and primary antibodies against pro-caspase-1 (ab207802) and caspase-1 (ab179515) were purchased from Abcam (MA, USA). Alexa Fluor 488

goat anti-rabbit IgG (AS054) and Alexa Fluor 594 goat anti-rabbit IgG (AS053) were obtained from ABclonal Technology (Wuhan, China). Primary antibodies against PCNA (BS1289), CD68 (BS6885), and β-actin (BS6007M) were purchased from Bioworld Technology, Inc. (St. Paul, MN, USA). The Pierce BCA protein assay kit and Triton X-100 were supplied by Thermo Fisher Scientific (CA, USA). Phorbol 12-myristate 13-acetate (PMA) was purchased from Promega Corporation (WI, USA). Murine GM-CSF was obtained from PeproTech (Suzhou, China).

2.2 Animals

Six-week-old male C57BL/6 mice were supplied by the Comparative Medicine Centre of Yangzhou University (Yangzhou, China). The mice were maintained in an animal laboratory under a 12-h light/dark cycle at an environmental temperature of 24 ± 2 ˚C, fed on standard chow pellets, and allowed access to water *ad libitum*. The mice were acclimatized for one week before the experiments. The animals were randomly assigned to experimental groups for the *in vivo* studies. Collection and evaluation of the data from the *in vivo* experiments were performed in a single-blind manner. The animal experiments were conducted with the approval of the Animal Ethics Committee of China Pharmaceutical University, and conformed to the National Institutes of the Health guidelines for the ethical use of animals.

2.3 Induction of CAC and treatments

Mice were given a single intraperitoneal injection of the azoxymethane (10 mg/kg) in combination with three cycles of 2% DSS in drinking water for one week, before the water containing DSS was replaced with regular drinking water for two weeks of

recovery (Fig. 1A). The mice were weighed each day[21, 22]. The mice were randomly divided into the following groups: the normal group, the AOM/DSS group, the arctigenin (25, 50 mg/kg) group, and the 5-aminosalicylic acid (5-ASA, mesalazine, 75 mg/kg) group. In the experiment to verify the role of carnitine palmitoyltransferase 1 (CPT1) in inflammasome activation and colon carcinogenesis, the mice were randomly divided into the following groups: the normal group, the adeno-associated virus (AAV)-control + AOM/DSS group, the AAV-control + arctigenin (25 mg/kg) group, the AAV-CPT1 + AOM/DSS group, the AAV-CPT1 + arctigenin (25 mg/kg) group, and the ETX (2 mg/kg) group. One week before the experiment began, AAV-CPT1 (Vigene Biosciences, Maryland, USA) overexpression and AAV-control were administered by enema. Arctigenin was suspended in 0.5% sodium carboxymethyl cellulose (CMC-Na), and AAV9-CPT1 plasmid virus and AAV9-control virus suspension (virus titer > 10^{13}) were diluted with normal saline, respectively. Arctigenin or mesalazine was administered orally once a day, and ETX was intraperitoneally injected every other day during the recovery period. The mice were euthanized 1 h after the final administration. Also, the mice in the normal and AOM/DSS groups were given an equal volume of vehicle (0.5 % CMC-Na).

2.4 Macroscopic assessment and histological analysis of colonic tissues

The distal sections of the colons of the mice were excised, fixed in 4% paraformaldehyde, and embedded in paraffin. The sections (5-μm thickness) were

stained with hematoxylin-eosin (H&E) and examined using a microscope (Olympus, Japan) at 200x magnification. The histological scores were calculated by a treatment-blind observer according to previously reported criteria[22].

2.5 Immunofluorescence of colon tissues

Briefly, the colon tissue sections were deparaffinized, rehydrated, and washed in phosphate-buffered saline (PBS). The sections were treated with 3% hydrogen peroxide and blocked with 3% bovine serum albumin (BSA) before incubation with primary antibody (1:100) for 1 h at room temperature. The slides were then counter-stained with DAPI for 30 min. The reaction was stopped by washing the slides with water for 5 min. Images were acquired with a fluorescence microscope (Olympus, Lake Success, NY).

2.6 Enzyme-linked immunosorbent assay (ELISA)

The mouse colons were homogenized with PBS. The homogenates were centrifuged at 12,000 × rpm at 4 °C for 15 min. The levels of TNF-α, IL-6, IL-17, IL-1β, and acetyl-CoA in the supernatants of colon homogenates were measured using ELISA kits according to the manufacturers' instructions. The IL-1β and acetyl-CoA levels in the differentiated THP-1 cells and bone marrow-derived macrophages (BMDMs) were measured using ELISA kits according to the manufacturers' instructions.

2.7 Cell culture

Human acute monocytic leukemia THP-1 cells, obtained from the Cell Bank of the

Chinese Academic of Sciences (Shanghai, China), were cultured in RPMI-1640 medium (Gibco, Carlsbad, USA), supplemented with 10% (v/v) fetal bovine serum (Gibco, Carlsbad, USA) and 0.05 mM 2-mercaptoethanol Sigma-Aldrich (St. Louis, USA). The cells were cultured in a humidified environment with 5% CO_2 at 37 °C. Differentiation of THP-1 cells was induced by stimulation with 0.5 mM PMA for 3 h. The differentiated cells were washed three times with PBS and treated with 1 μg/mL LPS in the absence or presence of arctigenin for 3 h, then stimulated with adenosine triphosphate (ATP, 5 mM) for 1 h. BMDMs were isolated from C57 BL/6 mice and cultured with Dulbecco's Modified Eagle Medium (DMEM, Gibco, Carlsbad, USA) supplemented with 10% (v/v) fetal bovine serum (Gibco, Carlsbad, USA) and 20 ng/mL GM-CSF. The cells were harvested and seeded on 6-well plates. The culture medium was changed every three days, and the adherent macrophages were obtained within approximately one week. After culture for 6 h without GM-CSF, the cells were washed three times with PBS and treated with 1 μg/mL LPS in the absence or presence of arctigenin for 3 h, then stimulated with ATP (5 mM) for 1 h.

2.8 MTT assay

The 3-(4,5-dimethylthiazol-2-yl)-2,5-diphenyl tetrazolium bromide (MTT, St. Louis, MO, USA) assay was performed to detect the cell viability of THP-1 cells and BMDMs in the presence of arctigenin. Briefly, THP-1 cells or BMDMs (1×10^4 cells per well) were seeded in 96-well culture plates and treated with arctigenin for 20 h.

Then, 20 μL of MTT (5 mg/mL) was added, and the cells were incubated for an additional 4 h at 37 °C. The medium was then removed carefully to avoid destroying the formazan crystals formed. DMSO was added to each well, and a microplate reader (Thermo Fisher Scientific, Waltham, Massachusetts, USA) was used to read the absorbance of the dissolved formazan at a wavelength of 570 nm.

2.9 Apoptosis analysis

THP-1 cells and BMDMs were treated as described above. The cells were cultured with or without arctigenin for 24 h, and then detached, washed, and stained with Annexin-V/PI (ROCHE) according to the manufacturer's instructions. The cell samples were analyzed with the FACSCalibur flow cytometer (Becton, Dickinson and Company, NJ, USA). The data were analyzed with FlowJo software (Tree Star).

2.10 Western blotting

The cells and colonic tissues were lysed on ice for 30 min in NP-40 buffer containing protease inhibitor cocktail (1:100), and then incubated for 30 min on ice. The homogenates were centrifuged, and the protein concentrations were determined using a Pierce BCA protein assay kit. Samples (10 μg) of total protein were subjected to sodium dodecyl sulphate–polyacrylamide gel electrophoresis (SDS-PAGE) analysis. The protein was transferred from the gel to the membranes, which were subsequently blocked with 5% (w/v) skimmed milk for 2 h, and incubated with specific primary antibodies overnight at 4 °C. Next, the membranes were incubated with IRDye-conjugated secondary antibody for 1 h at 37 °C. Detection was performed using the Odyssey Infrared Imaging System (LI-COR, Inc., Lincoln, USA).

2.11 Co-immunoprecipitation assay

THP-1 cells or BMDMs were lysed on ice in RIPA lysis buffer for 15 min, and then centrifuged at 12, 000 rpm for 5 min. The supernatants were collected and incubated with the antibody against NLRP3 overnight at 4 °C with constant rotation. The next day, the cocktails were incubated with the protein A+G beads for 4 h at room temperature with constant rotation. The precipitant was collected through centrifugation at 5 000 rpm for 5 min, and then washed 3 times with RAPI lysis buffer to remove non-specific binding proteins. The washed beads were re-suspended with loading buffer and heated at 95 °C for 5 min. The beads were removed by centrifugation at 12 000 rpm for 1 min. The immunoprecipitated proteins were prepared for western blotting.

2.12 Quantitative real-time PCR

Total RNA was extracted from the colon tissues and cells with Trizol reagent according to the manufacturer's instructions. Total RNA was reverse transcribed using the 5X All-In-One RT MasterMix (Abm, Zhengjiang, China). Real-time polymerase chain reaction (PCR) was performed with BrightGreen Express 2X qPCR MasterMix (Abm, Zhengjiang, China) on a Bio-rad IQ5 (Hercules, USA). The level of mRNA was normalized to the expression of β-actin. The results were analyzed using the $2^{-\Delta\Delta Ct}$ method. The primer sequences for the analyzed genes are listed in Tables 1 and 2.

Table 1. Mouse primer pairs used in real-time polymerase chain reaction.

Gene	Sequence (5'-3')	Length (bp)

Name/ID		
Il1b	Forward	tgccacctttgacagtgatg (21)
(Gene ID: 16176)	Reverse	tgtgctgctgcgagatttga (21)
Tnf	Forward	ccctcacactcacaaaccac (20)
(ID: 21926)	Reverse	acaaggtacaacccatcggc (20)
Il6	Forward	cacatgttctctgggaaatcg (21)
(Gene ID: 16193)	Reverse	cacatgttctctgggaaatcg (21)
Ptgs2	Forward	cccccacagtcaaagacact (20)
(Gene ID: 19225)	Reverse	atcatcagaccaggcacca (19)
Nos2	Forward	agggaatcttggagcgagtt (20)
(Gene ID: 18126)	Reverse	gcagcctcttgtctttgacc (20)
Il17a	Forward	ggactctccaccgcaatgaa (20)
(Gene ID: 16171)	Reverse	tttccctccgcattgacaca (20)
Actb	Forward	agcaagcaggagtacgatgag (21)
(Gene ID: 11461)	Reverse	ggtgtaaaacgcagctcagtaa (22)
Nlrp3	Forward	ccacatctgattgtgttaatggct (24)
(Gene ID: 216799)	Reverse	gggcttaggtccacacagaa (20)
Cpt1a	Forward	ctccgcctgagccatgaag (19)
(Gene ID: 12894)	Reverse	caccagtgatgatgccattct (21)

238

239 Table 2. Human primer pairs used in real-time polymerase chain reaction.

Gene Name/ID	Sequence (5'-3')	Length (bp)
IL1B	Forward	TGGTGGTCGGAGATTCGTA (19)
(Gene ID: 3553)	Reverse	TGGCAATGAGGATGACTTGT (20)
TNF	Forward	CTGAGTCGGTCACCCTTCTC (20)
(Gene ID: 7124)	Reverse	AACCTCCTCTCTGCCATCAA (20)
ACTB	Forward	CATGTACGTTGCTATCCAGGC (21)
(Gene ID: 60)	Reverse	CTCCTTAATGTCACGCACGAT (21)
NLRP3	Forward	GCATTTCCTCTCTAGCTGTTCCT (23)
(Gene ID: 114548)	Reverse	TTAGGCTTCGGTCCACACAGAAAG (24)
CPT1A	Forward	ATCAATCGGACTCTGGAAACGG (22)
(Gene ID: 1374)	Reverse	TCAGGGAGTAGCGCATGGT (19)

240

241 **2.13 Transient transfection**

242 The transfection of CPT plasmid was performed by using Hieff Trans^{TM} Liposomal
243 Transfection Reagent (Yeasen Biotech Co., Ltd. Shanghai, China) at a final
244 concentration of 50 nM according to the manufacturer's instructions. The transfection
245 efficiency was assessed by using quantitative PCR (qPCR) analysis 24 h after
246 transfection. Subsequently, the THP-1 cells or BMDMs were prepared for further
247 analysis.

248 **2.14 Immunofluorescence staining**

Cells were plated and cultured on plates. After treatment as mentioned above in the cell culture section, THP-1 cells or BMDMs were fixed with 4% paraformaldehyde for 15 min and permeabilized with 0.5% Triton X-100 for 15 min. Then, to minimize background staining, the cells were blocked with 5% BSA for 1 h at room temperature. The cells were incubated with the appropriate primary antibodies overnight at 4 °C. After being washed with PBS, the cells were washed and incubated with fluorescent secondary antibody and DAPI. The images were captured by a fluorescence microscope (Olympus BX51).

2.15 Measurement of CPT-1 activity

CPT-1 activity was measured in a buffer containing 100 mM Tris/HCl, pH 8.0, 0.1% Triton X-100, 1 mm EDTA, 0.01 mM palmitoyl-CoA, and 0.5 mM dithiobis-2-nitrobenzoic acid (DTNB), with or without 1.25 mM L-carnitine. The absorbance was read at 412 nm with a spectrophotometer[23]. CPT-1 activity was calculated as the difference between the rates in the presence and absence of L-carnitine, and expressed as nanomoles of CoA released per minute per 10^4 cells.

2.16 Liquid chromatography-mass spectrometry (LC-MS) metabolomic analysis

Extraction of metabolites: THP-1 cells (2×10^7 cells/sample) were transferred into 1.5-mL tubes with 1000 μL of extraction solvent (methanol: acetonitrile: water= 2:2:1 v/v/v, which was kept at -20 □ before extraction). The samples were homogenized in a ball mill for 4 min at 45Hz, then treated with ultrasound for 5 min (in ice water).

The samples were homogenized three times, and incubated at -20 °C for 1 h for protein precipitation. Following that, the samples were centrifuged at 12000 rpm for 15 min at 4 °C. The supernatants (825 μL) were transferred into 1.5-mL tubes, and dried in a vacuum concentrator without heating. After that, 100 μL extraction solvent (acetonitrile: water = 1:1 v/v) was added into the tubes. The samples were vortexed for 30 s and sonicated for 10 min at 4 °C, then centrifuged for 15 min at 12000 rpm at 4 °C. The supernatants (60 μL) were transferred into fresh 2-mL liquid chromatography–mass spectrometry (LC-MS) glass vials. Finally, 10 μL of supernatant from each sample was taken for quality control (QC), and 60 μL of supernatant was taken for UHPLC-QTOF-MS analysis.

LC-MS/MS analysis: the LC-MS/MS analysis was performed using an UHPLC system (1290, Agilent Technologies) with a UPLC BEH Amide column (1.7 μm 2.1*100 mm, Waters) coupled to TripleTOF 6600 (Q-TOF, AB Sciex). The mobile phase consisted of 25 mM NH_4OAc and 25 mM NH_4OH in water (pH = 9.75) (A) and acetonitrile (B) was carried with elution gradient as follows: 0 min, 95% B; 7 min, 65% B; 9 min, 40% B; 9.1 min, 95% B; 12 min, 95% B, which was delivered at 0.5 mL/min. The injection volume was 2 μL. The TripleTOF mass spectrometer was used due to its ability to acquire MS/MS spectra on an information-dependent basis (IDA) during an LC/MS experiment. In this mode, the acquisition software (Analyst TF 1.7, AB Sciex) continuously evaluates the full scan survey MS data as it collects and triggers the acquisition of MS/MS spectra depending on preselected criteria. In each

cycle, 12 precursor ions with an intensity greater than 100 were chosen for fragmentation at a collision energy (CE) of 30 V (15 MS/MS events with a product ion accumulation time of 50 msec each). The electrospray ionization (ESI) source conditions were set as follows: Ion source gas 1 as 60 Psi, Ion source gas 2 as 60 Psi, Curtain gas as 35 Psi, source temperature 650 °C, Ion Spray Voltage Floating (ISVF) 5000 V or -4000 V in positive or negative modes, respectively.

Data preprocessing and annotation: the MS raw data files were converted to mzXML format using ProteoWizard, and processed by R package XCMS (version 3.2). The preprocessing results generated a data matrix that comprised the retention time (RT), mass-to-charge ratio (m/z) values, and peak intensity. After XCMS data processing, R package CAMERA was used for peak annotation. An in-house MS2 database was applied for metabolite identification. An internal standard normalization method was also employed in this data analysis. The resulting three-dimensional data involving the peak number, sample name, and normalized peak area were entered into MetaboAnalyst (http://www.metaboanalyst.ca) for principal component analysis (PCA) and orthogonal projections to latent structures discriminate analysis (OPLS-DA). PCA showed the distribution of origin data. To obtain a higher level of group separation and a better understanding of the variables responsible for classification, supervised OPLS-DA was applied. Afterwards, the parameters for the classification from the software were R^2Y and Q^2Y, which were stable and good for fitness and prediction. Sevenfold cross-validation was used to estimate the robustness

and predictive ability of our model. A permutation test was performed to further validate the model. The low values of the Q^2Y intercept indicated the robustness of the models, showing a low risk of overfitting and reliability.

2.17 Fatty acid oxidation (FAO) assay

For the fatty acid oxidation (FAO) assay, THP-1 cells (5×10^4 cells/well) were plated on XF96 cell culture microplates (101085-004, Seahorse Bioscience). The oxygen consumption rate (OCR), as the parameter of mitochondrial FAO, was measured with a Seahorse XF96 bioanalyzer using the XF palmitate-BSA FAO substrate (Seahorse Bioscience, Agilent, USA) and Mito Stress Test Kit (Seahorse Bioscience, Agilent, USA) according to the manufacturer's instructions. The OCR for oxidation of palmitate-BSA was measured in THP-1 cells treated with palmitate-BSA (180 μM), etomoxir (40 μM), oligomycin (1.5 μM), and carbonyl cyanide 4-(trifluoromethoxy) phenylhydrazone (FCCP, 2 μM).

2.18 Statistical analysis

All data were expressed as mean ± standard error of the mean (S.E.M.). The differences between multiple groups were compared by one-way analysis of variance (ANOVA) followed by Tukey's test (SPSS, Chicago, USA). The correlation between two variables was evaluated by Spearman's nonparametric correlation analysis. $P < 0.05$ was considered to be statistically significant.

3. Results

3.1 Arctigenin prevented tumorigenesis in mice with CAC

To assess whether arctigenin can decrease the severity and incidence of CAC, we established an AOM/DSS mouse model via an intraperitoneal injection of carcinogenic AOM followed by three cycles of 2% DSS in drinking water (Fig. 1A). The survival rate of the mice in the AOM/DSS model group was 75%. All of the mice (100%) in the arctigenin-treated group survived (Fig. 1B). The body weights of the mice were monitored throughout the experiment. After each exposure to 2% DSS, the mice showed a substantial reduction in body weight but regained the weight after being given normal drinking water. The mice in the arctigenin (25, 50 mg/kg) treatment groups lost less weight after each DSS exposure and made a quicker recovery than the mice in the AOM/DSS group (Fig. 1C).

All mice were sacrificed in the 15th week after the induction of CAC. The incidence of tumors was 100% in all groups of mice except the normal group. As shown in Figure 1D, the mean colon length of the mice in the AOM/DSS group was slightly shorter than that of the normal group mice. Fewer and smaller tumors were seen in the mice treated with arctigenin (25, 50 mg/kg) or with 5-ASA (75 mg/kg). The macroscopic assessment of the mouse colons showed that arctigenin decreased the number of tumors and average tumor load, and resulted in smaller tumors (Fig. 1E-G). Histopathological examination revealed that the colons of the mice in the AOM/DSS group exhibited large adenocarcinomas inside the mucosa, with abnormal glands, expanding lumens, and infiltration of inflammatory cells. Arctigenin significantly ameliorated pathological changes, including mucosal damage, necrosis, and infiltration of inflammatory cells, and also reduced the number and size of adenocarcinomas inside the mucosa and decreased the number of abnormal cells (Fig. 1H).

On the other hand, proliferating cell nuclear antigen (PCNA) is involved in eukaryotic DNA replication. Tumor cells exhibit vigorous proliferation activity, and PCNA can be used as an indicator of cell proliferation status. CD68, a type I transmembrane glycoprotein, is a pan-marker of macrophages. Immunochemistry staining showed that the numbers of $PCNA^+$ cells and $CD68^+$ cells in the colon tissues of mice in the AOM/DSS group were significantly increased compared with those in the colon tissues of the normal group, while arctigenin treatment decreased the numbers of $PCNA^+$ cells and $CD68^+$ cells (Fig. 1I, J). Together, these results indicated that arctigenin administration reduced colitis-associated tumorigenesis in mice.

3.2 Arctigenin suppressed IL-1β maturation in the colonic macrophages of mice with CAC

In the past decade, many studies have demonstrated that macrophages aggravate inflammation and drive tumorigenesis and progression by secreting pro-inflammatory cytokines[7, 8, 24]. To study the underlying mechanisms by which arctigenin protects against CAC, we observed the expression of inflammatory cytokines in the colonic tumor tissues of mice. Figure 2A shows that the mRNA expression levels of tumor necrosis factor α (TNF-α), interleukin 17A (IL-17A), inducible nitric oxide synthase (iNOS), cyclo-oxygenase (COX2), interleukin-1β (IL-1β), and interleukin-6 (IL-6) were significantly increased in the colon tissues of the AOM/DSS-treated mice. Arctigenin at 25 and 50 mg/kg remarkably inhibited the mRNA expression of TNF-α, IL-17A, iNOS, and IL-1β. ELISA confirmed that the protein expression of TNF-α, IL-17A, and IL-1β was also inhibited by arctigenin (Fig. 2B). The inhibitory potency of arctigenin on IL-1β expression was significantly stronger than the effect it exerted on other proinflammatory cytokines. As the enhanced expression of cleaved IL-1β is an indicator of inflammasome activation[25], the mouse colon tissue sections were stained to detect inflammasome activation. Immunofluorescence assay showed a significantly increased number of $CD68^+$ $NLRP3^+$ macrophages in the colon tissues

of AOM/DSS-treated mice, which could be restrained by arctigenin treatment (Fig. 2C).

Additionally, we further determined the NLRP3 inflammasome complex protein in the colon tissues. The protein expression of caspase-1 in the AOM/DSS model group mice was found to be strongly enhanced compared to that in the mice in the normal control group. In the arctigenin-treated groups, the levels of NLRP3 and pro-caspase-1 were still at elevated levels; however, the levels of cleaved caspase-1 and cleaved IL-1β decreased (Fig. 2D). These data showed that arctigenin inhibited the expression of proinflammatory cytokines in the colonic macrophages of the mice with CAC, especially that of IL-1β, by suppressing NLRP3 inflammasome activation.

3.3 Arctigenin disrupted NLRP3 inflammasome assembly in macrophages

To uncover the mechanisms by which arctigenin suppresses NLRP3 inflammasome activation in the colon macrophages of CAC mice, we explored the impact of arctigenin on the inflammatory activation of cultured macrophages stimulated with LPS/ATP *in vitro*. Arctigenin (3, 10, and 30 μM) showed concentration-dependent inhibition of the secretion of IL-1β and IL-18 from LPS/ATP-treated THP-1 cells and BMDMs, with no clear impact on the survival of macrophages (Fig. 3A-D and Supplementary Figure 1A-D). These results were further confirmed by the detection of the p17 fragment of mature IL-1β. Moreover, the activation of caspase-1 in macrophages, as indicated by the presence of the cleaved form and enzyme activity, was significantly inhibited by arctigenin (3, 10, and 30 μM) (Fig. 3E and Supplementary Figure 1E). Furthermore, immunoprecipitation and immunofluorescence analyses showed that arctigenin also disrupted the process of NLRP3 inflammasome formation (Fig. 3F, G and Supplementary Figure 1F, G). The inhibitory effect of arctigenin on NLRP3 inflammasome assembly was significantly stronger than that on NLRP3 mRNA expression (Fig. 3H and Supplementary Figure

1H), indicating that arctigenin inhibited NLRP3 inflammasome activation mainly by disrupting assembly rather than interfering with the expression of NLRP3, ASC, pro-caspase 1, or pro-IL-1β.

3.4 Arctigenin downregulated FAO, but not glycolysis, during NLRP3 inflammasome assembly in macrophages

Increasing evidence suggests that cellular metabolism, in particular the processes of glycolysis, FAO, and amino acid metabolism, plays a critical role in NLRP3 inflammasome activation by providing intermediates for inflammasome assembly[26-28]. We measured the metabolite profiles of THP-1 cells stimulated with LPS/ATP using an untargeted UHPLC-QTOFMS-based metabolomics technique to identify which cellular metabolism pathway, if any, is involved in arctigenin activity against NLRP3 inflammasome assembly in macrophages. The typical LC-MS total ion current (TIC) chromatograms of the cell samples in both positive and negative modes are shown in Figure 4A. The QC samples were selected according to polarity and intensity to assess the repeatability and stability of the system. The results (Supplementary Figure 2) showed that the established method was repeatable and stable. There were 1169 peaks in the positive ion mode and 663 peaks in the negative ion mode. Principal components analysis (PCA) was implemented to investigate the metabolic changes among the three groups. The normal group and the LPS/ATP group were completely separated, and the arctigenin group was trending towards the normal group (Fig. 4B). The metabolites potentially contributing to the sample classification were shown by OPLS-DA (Fig. 4C). Variables with VIP >1.0 and *P* value < 0.05 were regarded as candidate metabolites. As shown in Supplementary Figure 3, 23 variables were predicted by comparing the correct MS and MS/MS fragments with the metabolites found through database searches. To further evaluate the effects of arctigenin on these potential biomarkers, the relative peak areas of the 25 metabolites to their respective total integrated area of the spectra were investigated and visualized by heatmap (Fig.

4D). The results showed that the contents of 31 metabolites were reversed by arctigenin treatment (Fig. 4E). In the LPS/ATP group, FAO-relevant metabolites, including palmityl-CoA, pyrophosphate, stearic acid, stearoyl-CoA, stearoyl carnitine, tetradecanoyl-CoA, oleic acid, and linoleic acid, were elevated, while 5 of them were reversed by arctigenin treatment. Fructose 6-phosphate and glucose 6-phosphate were elevated in the LPS/ATP group; however, arctigenin had no significant influence on these metabolites. The metabolic network of these potential biomarkers was established and is displayed in Fig. 4F. These results highlight the fact that both FAO and glycolysis were upregulated by LPS/ATP stimulation, while arctigenin selectively downregulated FAO, in macrophages.

To further evaluate the effect of arctigenin on FAO, we detected the level of acetyl-CoA, which is mainly produced by β-oxidation of fatty acids, in THP-1 cells and BMDMs (Fig. 5A and Supplementary Figure 4A). The production of acetyl-CoA in THP-1 cells and BMDMs was higher after stimulation with LPS/ATP. Moreover, arctigenin treatment (3, 10, and 30 μM) resulted in a significant reduction of acetyl-CoA production and inhibited the palmitate-induced increase in the oxygen consumption rate (OCR) in cultured THP-1 cells and BMDMs (Fig. 5B and Supplementary Figure 4B). In contrast, the extracellular acidification rate (ECAR) remained constant whether arctigenin was present or not (Fig. 5C and Supplementary Figure 4C). Together, these results suggested that arctigenin downregulated FAO, but not glycolysis, in THP-1 cells and BMDMs.

3.5 Arctigenin disrupted NLRP3 inflammasome assembly in macrophages depending on the downregulation of CPT1 expression

Previous studies have indicated that the knockout of CPT1, the rate-limiting enzyme in FAO, can inhibit NLRP3 inflammasome activation[27]. To investigate the

involvement of CPT1 in arctigenin-mediated inhibition of NLRP3 inflammasome assembly in macrophages, we assessed the effects of arctigenin on the activity and expression of CPT1. Figure 5D and Supplementary Figure 4D show that the activity of CPT1 in THP-1 cells and BMDMs did not change after arctigenin treatment. The CPT1 mRNA and protein expression levels (Fig. 5E, F and Supplementary Figure 4E, F) were increased in LPS/ATP-stimulated THP-1 cells and BMDMs; however, these effects were suppressed by arctigenin (3, 10, 30 μM). To ascertain the role of CPT1 in the response of macrophages to LPS/ATP, we created THP-1 cells overexpressing CPT1. The transfection efficiency of CPT1 plasmid was validated by qPCR (Fig. 6A), and the enhancement of FAO after CPT1 overexpression was assessed by detecting the production of acetyl-CoA (Fig. 6B). CPT1 overexpression drove NLRP3 inflammasome assembly and resulted in ASC oligomerization, enhanced caspase-1 activation, and IL-1β cleavage (Fig. 6C-E) relative to the control plasmid in LPS/ATP-stimulated THP-1 cells. Moreover, the inhibitory effects of arctigenin on NLRP3 inflammasome assembly, ASC oligomerization, caspase-1 activation, and IL-1β cleavage were almost completely reversed by the overexpression of CPT1 in THP-1 cells compared to the controls. We, therefore, speculate that the downregulation of CPT1 expression to weaken FAO is responsible for the effect of arctigenin on the prevention of NLRP3 inflammasome assembly in macrophages.

3.6 Arctigenin disrupted NLRP3 assembly through the inhibition of α-tubulin acetylation *via* downregulating CPT1 expression

In FAO metabolism, fatty acid β oxidation is split stepwise into two-carbon fragments forming acetyl-CoA[29]. Acetyl-CoA is the major direct acetyl donor for acetylation in the biological system[30]. The inhibition of α-tubulin acetylation has recently been reported to mediate the spatial arrangement of mitochondria and cause the insufficient

assembly of ASC with NLRP3 in the mitochondria[31]. To further dissect how arctigenin downregulates the expression of CPT1 to influence the NLRP3 assembly in macrophages, we measured the expression of α-tubulin and acetylated α-tubulin in macrophages. As shown in Figure 7A, arctigenin (3, 10, and 30 μM) did not impact the expression of total α-tubulin; in contrast, it significantly inhibited the acetylation of α-tubulin in LPS/ATP-challenged THP-1 cells.

Further, we performed immunofluorescence analysis of acetylated α-tubulin proteins and ASC in THP-1 cells. Of note, CPT1 overexpression strongly enhanced the acetylation of α-tubulin, and dramatically weakened the inhibitory effect of arctigenin (10 μM) on the expression of acetylated α-tubulin in THP-1 cells (Fig. 7B). The data revealed that arctigenin reduced colocalization between acetylated α-tubulin and ASC (Fig. 7C). These findings show that arctigenin disrupted NLRP3 assembly through inhibition of α-tubulin acetylation in macrophages via downregulating CPT1 expression.

3.7 Downregulation of FAO contributed to the inhibitory effect of arctigenin on NLRP3 inflammasome activation and tumorigenesis in mice with CAC

To determine whether the anti-CAC effect of arctigenin was linked to the downregulation of CPT1-mediated FAO, we used AAV-9 as a vehicle to specifically overexpress CPT1 in the colons of CAC mice administered with either arctigenin (25 mg/kg) or vehicle for 15 weeks commencing the first week after AOM injection. The transfection efficiency of AAV-CPT1 was validated by qPCR (Supplementary Figure 5A), and the enhancement of FAO after the overexpression of CPT1 was assessed by detecting the production of acetyl-CoA (Supplementary Figure 5B). The mice with CPT1 overexpression had a more dramatic reduction in survival (Fig. 8A), body weight (Fig. 8B), and shortening of colon length (Fig. 8C). The number, load, and size of the tumors in mice with CPT1 overexpression showed statistically significant

increases compared with those in the vehicle group mice (Fig. 8D-F). Histopathological examination revealed that the colons of the mice in the AOM/DSS group and AOM/DSS with CPT1 overexpression group had large adenocarcinomas inside the mucosa. Also, the mice in the AOM/DSS and AOM/DSS with CPT1 overexpression groups showed an inflammatory response and crypt loss (Fig. 8G). The numbers of $CD68^+$ $NLRP3^+$ macrophages were significantly increased in the AOM/DSS group and AOM/DSS with CPT1 overexpression group (Fig. 8H). Figure 8I shows that CPT1 overexpression strongly increased the expression of IL-1β, while also promoting α-tubulin acetylation and acetyl-CoA production in the colon tissues (Supplementary Figure 5B, C). As anticipated, arctigenin treatment was ineffective against AOM/DSS-induced tumor progression, as well as against macrophage and NLRP3 inflammasome activation, which demonstrated that the inhibitory effect of arctigenin on NLRP3 inflammasome activation in colonic macrophages and CAC disappeared with CPT1 overexpression in colon tissues. Positive correlations were found between CPT1 mRNA expression and tumor number, tumor size, tumor load, pathological score, and IL1β expression by Spearman's correlation analysis (Fig. 9 A-E). Taken together, these results demonstrate that arctigenin exerts an anti-CAC effect primarily through the downregulation of CPT1 expression and consequent NLRP3 inflammasome activation in colonic macrophages, and, thus, uncover the critical role of CPT1 in inflammasome activation and the progression of colon carcinogenesis.

4. Discussion

CRC is a devastating gastrointestinal cancer with high morbidity and mortality[1, 2]. Multiple risk factors, including an unhealthy diet, smoking, obesity, and environmental factors, can enhance the incidence of CRC. Among these risk factors, chronic non-resolving inflammation in IBD individuals has been acknowledged to contribute to the initiation and progression of CRC, and anti-inflammatory interventions can help to prevent the development of CAC[32]. Arctigenin, a lignin constituent isolated from Fructus Arctii, has been reported to inhibit the proliferation of various tumor cells, especially pancreatic cancer cells, and the growth of xenograft tumors[16-18]. Our earlier studies proved that arctigenin could attenuate colon inflammation in mice with DSS-induced colitis[15], suggesting its potential benefits for the prevention and treatment of CRC. In the present study, we investigated the anti-CAC potential of arctigenin and the underlying mechanism. The results showed that orally administered arctigenin markedly inhibited AOM/DSS-induced CAC in mice, as evidenced by tumor number, size, burden, and histopathological examination.

The mechanism by which chronic inflammation drives tumor development is complex, and various proinflammatory cytokines might play important roles. Among them, IL-1β has attracted much attention. IL-1β can propagate the initial mutations and cause a cascade of inflammatory responses and tissue damage by modulating the function of dendritic cells, neutrophils, and T cells. IL-1β can also rescue initiated tumor cells from apoptosis and enable their proliferation, leading to a malignant

phenotype[33]. In this study, arctigenin significantly inhibited the secretion of various proinflammatory cytokines from the colonic macrophages of CAC model mice, with the most active inhibition on IL-1β secretion. This observation implies that the anti-CAC effect of arctigenin might be linked to the inhibition of IL-1β secretion. Furthermore, arctigenin was previously reported to ameliorate DSS-induced colitis in mice by down-regulating Th17 cell response[15]. Given that IL-1β can induce the differentiation and maintenance of Th17 cells and Th1/Th17 expansion/activation can recruit myeloid leukocytes to the colon and aggravate inflammation[34-36], further studies are needed to validate the importance of IL-1β in arctigenin's attenuation of colitis.

IL-1β is well known to only be active in an inflammasome-dependent processed and secreted form[37]. The formation of inflammasome might be triggered by diverse microorganisms and their products or by stress-associated signals that support the autocatalytic cleavage of pro-caspase-1, which is activated on the inflammasome platform, and subsequently cleaves the inactive precursors of IL-1β (31 kD) into their mature secreted 17 kD form[38]. Interestingly, arctigenin did not affect the expression of the precursors of IL-1β and caspase-1; however, it significantly reduced the mature IL-1β and cleaved caspase-1 *in vivo* and *in vitro*. In macrophages, NLRP3 inflammasome activation is a two-step process. The first step is priming, which usually controls the transcriptional synthesis of relevant genes such as pro-IL-1β, NLRP3, and ASC[39]. The second step is activation, which provokes the assembly of the NLRP3 inflammasome[40]. Pu et al. reported that arctigenin with the addition of LPS could inhibit the expression of NLRP3 protein in THP-1 cells[41]. In contrast, our results showed that arctigenin, added at 3 h after LPS stimulation, did not affect the mRNA and protein expression of NLRP3, but significantly impeded the formation of ASC oligomerization as well as the process of NLRP3 inflammasome assembly. It is likely that arctigenin directly interferes with the NLRP3 inflammasome assembly

process in macrophages. Further, we investigated the effect of arctigenin on the NLRP3 inflammasome assembly process in murine bone-marrow-derived neutrophils. The results showed that arctigenin decreased ASC oligomer formation and IL-1β production (Supplementary Figure 6). In the colons of CRC patients[42] and CAC mice, the infiltration of macrophages is more obvious than that of neutrophils (data not shown). We employed macrophages in an *in vitro* model to investigate the mechanism by which arctigenin inhibited NLRP3 inflammasome assembly.

Several metabolic intermediates appear to be involved in the assembly of the NLRP3 inflammasome in macrophages. A shift in our understanding of NLRP3 inflammasome assembly has occurred because of recent discoveries around the metabolic reprogramming of macrophages[43]. Along with the sensing of cell metabolic changes, increased fatty acid oxidation, amino acid influx, and glycolysis, have recently emerged as additional critical activators of inflammasome assembly[44, 45]. The NLRP3 inflammasome has been shown to sense metabolites such as palmitate, uric acid, and cholesterol crystals, but it is inhibited by ketone bodies produced during metabolic flux[46]. Metabolic reprogramming in macrophages appears to provide vital energy and substrates supplement steps in NLRP3 assembly shared by several stimuli, including ATP and nigericin. In this study, we found that the levels of acetyl-CoA were higher in response to LPS/ATP or LPS/palmitate-BSA in THP-1 and BMDMs compared to those in normal controls. The oxidation of fatty acids generates acetyl-CoA, which fuels NLRP3 inflammasome assembly. During NLRP3 inflammasome assembly, acetyl-CoA acts as an acetyl donor for α-tubulin acetylation. The acetylated-α-tubulin interacts with ASC to form oligomers and contributes the assembly of the NLRP3 inflammasome[47]. Arctigenin and etomoxir were shown to downregulate FAO, suppress α-tubulin acetylation, and eventually hinder NLRP3 inflammasome assembly in macrophages. FAO is essential for energy homeostasis and is regulated by CPT1[48]. Here, we employed CPT1 overexpression plasmid to

613 enhance the FAO in macrophages and demonstrated that CPT1-dependent FAO is
614 required for arctigenin's inhibition of NLRP3 inflammasome assembly. The findings
615 obtained from our *in vitro* studies were verified in AOM/DSS-induced CAC mice.
616 The inhibitory effect of arctigenin on the expression of CPT1 was positively
617 correlated with the reduction of tumor size, tumor number, and tumor burden in CAC
618 mice.

619 In conclusion, the results of this study confirm the protective effect of arctigenin
620 against CAC in mice through inhibiting inflammation. The action mechanism of
621 arctigenin involves FAO-dependent stunting of NLRP3 inflammasome assembly and
622 activation, thus leading to decreased IL-1β secretion by macrophages. Furthermore,
623 CPT1-mediated FAO was demonstrated to be a potential pharmacologic target of
624 NLRP3 activation and CAC. The findings presented here may help guide decisions
625 regarding the use of arctigenin as an anti-inflammatory agent in IBD patients to
626 reduce the risk of CAC.
627

Acknowledgments

This work was supported by the China National Natural Science Foundation (No. 81673666, 81874361), “Double First-Class” University project [CPU2018GY10] and Postgraduate Research & Practice Innovation Program of Jiangsu Province [KYCX18_0821].

Conflicts of interest

The authors have no conflicts of interest to declare.

References

1. Global Burden of Disease Cancer Collaboration, Fitzmaurice C, Abate D, et al. Global, regional, and national cancer incidence, mortality, years of life lost, years lived with disability, and disability-adjusted life-years for 29 Cancer Groups, 1990 to 2017: a systematic analysis for the global burden of disease study. JAMA Oncol, 2019 Sep 27. DOI: 10.1001/jamaoncol.2019.2996. [Epub ahead of print]

2. Bray F, Ferlay J, Soerjomataram I, et al. Global cancer statistics 2018: GLOBOCAN estimates of incidence and mortality worldwide for 36 cancers in 185 countries. CA: A Cancer Journal for Clinicians, 2018, 68: 394-424. DOI: 10.3322/caac.21492

3. Cox SR, Lindsay JO, Fromentin S, et al. Effects of low-FODMAP diet on symptoms,fecal microbiome, and markers of inflammation in patients with quiescent inflammatory bowel disease in a randomized trial. Gastroenterology, 2020, 158: 176-188.e7. DOI: 10.1053/j.gastro.2019.09.024

4. Keum N, Giovannucci E. Global burden of colorectal cancer: emerging trends, risk factors and prevention strategies. Nature Reviews Gastroenterology & Hepatology, 2019, 16: 713-732. DOI: 10.1038/s41575-019-0189-8

653 5. Terzić J, Grivennikov S, Karin E, et al. Inflammation and colon cancer.
654 Gastroenterology, 2010, 138: 2101-2114. DOI: 10.1053/j.gastro.2010.01.058

655 6. Fumery M, Dulai PS, Gupta S, et al. Incidence, risk factors, and outcomes of
656 colorectal cancer in patients with ulcerative colitis with low-grade dysplasia: a
657 systematic review and meta-analysis. Clinical Gastroenterology and Hepatology, 2017,
658 15: 665-674. e5. DOI: 10.1016/j.cgh.2016.11.025

659 7. Guo H, Callaway JB, Ting JP. Inflammasomes: mechanism of action, role in
660 disease, and therapeutics. Nature Medicine, 2015, 21: 677-687. DOI:
661 10.1038/nm.3893

662 8. Zaki MH, Lamkanfi M, Kanneganti TD. The Nlrp3 inflammasome: contributions to
663 intestinal homeostasis. Trends in Immunology, 2011, 32: 171-179. DOI:
664 10.1016/j.it.2011.02.002

665 9. Voronov E, Apte RN. IL-1 in colon inflammation, colon carcinogenesis and
666 invasiveness of colon cancer. Cancer Microenvironment, 2015, 8: 187-200. DOI:
667 10.1007/s12307-015-0177-7

668 10. Apte RN, Dotan S, Elkabets M, et al. The involvement of IL-1 in tumorigenesis,
669 tumor invasiveness, metastasis and tumor-host interactions. Cancer Metastasis
670 Reviews, 2006, 25: 387-408. DOI: 10.1007/s10555-006-9004-4

671 11. Zaki MH, Boyd KL, Vogel P, et al. The NLRP3 inflammasome protects against
672 loss of epithelial integrity and mortality during experimental colitis. Immunity, 2010,
673 32: 379-391. DOI: 10.1016/j.immuni.2010.03.003

674 12. Bader JE, Enos RT, Velázquez KT, et al. Macrophage depletion using clodronate
675 liposomes decreases tumorigenesis and alters gut microbiota in the AOM/DSS mouse
676 model of colon cancer. American Journal of Physiology-Gastrointestinal and Liver
677 Physiology, 2018, 314: G22-G31. DOI: 10.1152/ajpgi.00229.2017

678 13. Seo SU, Kamada N, Muñoz-Planillo R, et al. Distinct commensals induce

679 interleukin-1β via NLRP3 inflammasome in inflammatory monocytes to promote
680 intestinal inflammation in response to injury. Immunity, 2015, 42: 744-755. DOI:
681 10.1016/j.immuni.2015.03.004

682 14. Spalinger MR, Manzini R, Hering L, et al. PTPN2 regulates inflammasome
683 activation and controls onset of intestinal inflammation and colon cancer. Cell
684 Reports, 2018, 22: 1835-1848. DOI: 10.1016/j.celrep.2018.01.052

685 15. Wu X, Dou Y, Yang Y, et al. Arctigenin exerts anti-colitis efficacy through
686 inhibiting the differentiation of Th1 and Th17 cells via an mTORC1-dependent
687 pathway. Biochemical Pharmacology, 2015, 96: 323-336. DOI:
688 10.1016/j.bcp.2015.06.008

689 16. Chen GR, Li HF, Dou DQ, et al. (-)-Arctigenin as a lead compound for anticancer
690 agent. Natural Product Research, 2013, 27: 2251-2255. DOI:
691 10.1080/14786419.2013.821120

692 17. Wang P, Solorzano W, Diaz T, et al. Arctigenin inhibits prostate tumor cell growth
693 in vitro and in vivo. Clinical Nutrition Experimental, 2017, 13: 1-11. DOI:
694 10.1016/j.yclnex.2017.04.001

695 18. Kim JY, Hwang JH, Cha MR, et al. Arctigenin blocks the unfolded protein
696 response and shows therapeutic antitumor activity. Journal of Cellular Physiology,
697 2010, 224: 33-40. DOI: 10.1002/jcp.22085

698 19. Fujioka R, Mochizuki N, Ikeda M, et al. Change in plasma lactate concentration
699 during arctigenin administration in a phase I clinical trial in patients with
700 gemcitabine-refractory pancreatic cancer. PloS one, 2018, 13: e0198219. DOI:
701 10.1371/journal.pone.0198219

702 20. Awale S, Lu J, Kalauni SK, Kurashima Y, et al. Identification of arctigenin as an
703 antitumor agent having the ability to eliminate the tolerance of cancer cells to nutrient
704 starvation. Cancer Research, 2006, 66: 1751-1757. DOI:

10.1158/0008-5472.can-05-3143

21. Parang B, Barrett CW, Williams CS. AOM/DSS model of colitis-associated cancer. Methods in Molecular Biology, 2016, 1422: 297-307. DOI: 10.1007/978-1-4939-3603-8_26

22. Neufert C, Becker C, Neurath MF. An inducible mouse model of colon carcinogenesis for the analysis of sporadic and inflammation-driven tumor progression. Nature Protocols. 2007, 2: 1998-2004. DOI: 10.1038/nprot.2007.279

23. Derdak Z, Villegas KA, Harb R, et al. Inhibition of p53 attenuates steatosis and liver injury in a mouse model of non-alcoholic fatty liver disease. Journal of Hepatology, 2013, 58: 785-791. DOI: 10.1016/j.jhep.2012.11.042

24. Koelzer VH, Canonica K, Dawson H, et al. Phenotyping of tumor-associated macrophages in colorectal cancer: Impact on single cell invasion (tumor budding) and clinicopathological outcome. Oncoimmunology, 2015, 5: e1106677. DOI: 10.1080/2162402X.2015.1106677

25. Snodgrass RG, Huang S, Choi IW, et al. Inflammasome-mediated secretion of IL-1β in human monocytes through TLR2 activation; modulation by dietary fatty acids. The Journal of Immunology, 2013, 191: 4337-4347. DOI: 10.4049/jimmunol.1300298

26. Shirasuna K, Takano H, Seno K, et al. Palmitic acid induces interleukin-1β secretion via NLRP3 inflammasomes and inflammatory responses through ROS production in human placental cells. Journal of Reproductive Immunology, 2016, 116: 104-112. DOI: 10.1016/j.jri.2016.06.001

27. Moon JS, Nakahira K, Chung KP, et al. NOX4-dependent fatty acid oxidation promotes NLRP3 inflammasome activation in macrophages. Nature Medicine, 2016, 22: 1002-1012. DOI: 10.1038/nm.4153

28. Zhang Q, Wang H, Mao C, et al. Fatty acid oxidation contributes to IL-1β

731 secretion in M2 macrophages and promotes macrophage-mediated tumor cell
732 migration. Molecular Immunology, 2018, 94: 27-35. DOI:
733 10.1016/j.molimm.2017.12.011

734 29. Kalucka J, Bierhansl L, Conchinha NV, et al. Quiescent endothelial cells
735 upregulate fatty acid β-oxidation for vasculoprotection via redox homeostasis. Cell
736 Metabolism, 2018, 28: 881-894. DOI: 10.1016/j.cmet.2018.07.016

737 30. Paik WK, Pearson D, Lee HW, et al. Nonenzymatic acetylation of histones with
738 acetyl-CoA. Biochimica et Biophysica Acta-Nucleic Acids and Protein Synthesis.
739 1970, 213: 513-522. DOI: 10.1016/0005-2787(70)90058-4

740 31. Misawa T, Saitoh T, Kozaki T, et al. Resveratrol inhibits the acetylated
741 α-tubulin-mediated assembly of the NLRP3-inflammasome. International
742 Immunology, 2015, 27: 425-434. DOI: 10.1093/intimm/dxv018

743 32. Lewis JG, Adams DO. Inflammation, oxidative DNA damage, and carcinogenesis.
744 Environmental Health Perspectives, 1987, 76: 19-27. DOI: 10.1289/ehp.877619

745 33. Kühl AA, Erben U, Kredel LI, et al. Diversity of intestinal macrophages in
746 inflammatory bowel. Frontiers in Immunology, 2015, 6: 613. DOI:
747 10.3389/fimmu.2015.00613

748 34. Zhang X, Wei L, Wang J, et al. Suppression colitis and colitis-associated colon
749 cancer by anti-S100a9 antibody in mice. Frontiers in Immunology, 2017, 8: 1774.
750 DOI: 10.3389/fimmu.2017.01774

751 35. Castro-Dopico T, Dennison TW, Ferdinand JR, et al. Anti-commensal IgG drives
752 intestinal inflammation and type 17 immunity in ulcerative colitis. Immunity. 2019,
753 50: 1099-1114.e10. DOI: 10.1016/j.immuni.2019.02.006.

754 36. Ryzhakov G, West NR, Franchini F, et al. Alpha kinase 1 controls intestinal
755 inflammation by suppressing the IL-12/Th1 axis. Nature Communications, 2018, 9:
756 3797. DOI: 10.1038/s41467-018-06085-5.

757 37. Chan AH, Schroder K. Inflammasome signaling and regulation of
758 interleukin-family cytokines. Journal of Experimental Medicine, 2020, 217(1). pii:
759 e20190314. DOI: 10.1084/jem.20190314

760 38. Swanson KV, Deng M, Ting JP. The NLRP3 inflammasome: molecular activation
761 and regulation to therapeutics. Nature Reviews Immunology, 2019, 19: 477-489. DOI:
762 10.1038/s41577-019-0165-0

763 39. Evavold CL, Kagan JC. Inflammasomes: threat-assessment organelles of the
764 innate immune system. Immunity, 2019, 51: 609-624. DOI:
765 10.1016/j.immuni.2019.08.005

766 40. Man SM. Inflammasomes in the gastrointestinal tract: infection, cancer and gut
767 microbiota homeostasis. Nature Reviews Gastroenterology & Hepatology, 2018, 15:
768 721-737. DOI: 10.1038/s41575-018-0054-1

769 41. Pu Z, Han C, Zhang W, et al. Systematic understanding of the mechanism and
770 effects of Arctigenin attenuates inflammation in dextran sulfate sodium-induced acute
771 colitis through suppression of NLRP3 inflammasome by SIRT1. American Journal of
772 Translational Research, 2019, 11: 3992□4009.

773 42. Ye L, Zhang T, Kang Z, et al. Tumor-infiltrating immune cells act as a marker for
774 prognosis in colorectal cancer. Frontiers in Immunology. 2019, 10: 2368. DOI:
775 10.3389/fimmu.2019.02368.

776 43. Kelley N, Jeltema D, Duan Y, et al. The NLRP3 inflammasome: An overview of
777 mechanisms of activation and regulation. International Journal of Molecular Sciences,
778 2019, 20: 3328. DOI: 10.3390/ijms20133328

779 44. Arbore G, Kemper C. A novel “complement-metabolism-inflammasome axis” as a
780 key regulator of immune cell effector function. European Journal of Immunology,
781 2016, 44: 1563-1573. DOI: 10.1002/eji.201546131

782 45. Hughes MM, O'neill LA. Metabolic regulation of NLRP3. Immunological

Reviews, 2018, 281: 88-98. DOI: 10.1111/imr.12608

46. Moon JS, Lee S, Park MA, et al. UCP2-induced fatty acid synthase promotes NLRP3 inflammasome activation during sepsis. Journal of Clinical Investigation, 2015, 125: 665-680. DOI: 10.1172/JCI78253

47. Misawa T, Takahama M, Kozaki T, et al. Microtubule-driven spatial arrangement of mitochondria promotes activation of the NLRP3 inflammasome. Nature Immunology, 2013, 14: 454-460. DOI: 10.1038/ni.2550

48. Qu Q, Zeng F, Liu X, et al. Fatty acid oxidation and carnitine palmitoyltransferase I: emerging therapeutic targets in cancer. Cell Death & Disease, 2016, 19: e2226. DOI: 10.1038/cddis.2016.132

Figure legends

Figure 1. Effect of arctigenin on colitis-associated cancer induced by AOM/DSS in mice. (A) Schematic of the AOM/DSS model of colitis-associated cancer. (B) Percent survival rate (d, days). (C) Percent weight change. (D) The length of the mouse colons. (E) The number of tumors in the mouse colon tissues. (F) The size of the tumors in the mouse colon tissues. (G) The tumor load in the mouse colon tissues. (H) The histological changes of the colon tissues were examined by using hematoxylin-eosin staining (Scale bar: 50 μm). (I) Infiltration by $PCNA^+$ cells was evaluated by immunohistochemistry. The positive cells are dyed in brown (Scale bar: 50 μm). (J) Infiltration by $CD68^+$ cells was evaluated by immunohistochemistry. The positive cells are dyed in brown (Scale bar: 50 μm). Data are presented as mean ±

S.E.M. n = 6-8. $^{\#}p < 0.05$ and $^{\#\#}p < 0.01$ *vs.* Normal group; $^{*}p < 0.05$ and $^{**}p < 0.01$ *vs.* AOM/DSS group.

Figure 2. Effect of arctigenin on the levels of inflammatory cytokines and NLRP3 inflammasome activation in the colons of mice with colitis-associated cancer.

(A) The mRNA levels of TNF-α, IL-17A, iNOS, COX2, IL-1β, and IL-6 were detected by q-PCR assay. (B) The levels of TNF-α, IL-17A, NO, COX2, IL-1β, and IL-6 were measured by ELISA. (C) The infiltration of $CD68^{+}$ $NLRP3^{+}$ cells in the mouse colon tissues was evaluated by immunofluorescence histochemistry (Scale bars: 100 μm). (D) The protein levels of NLRP3, ASC, pro-caspase 1, caspase 1, pro-IL-1β, and IL-1β were examined by western blot. Data are presented as mean ± S.E.M. n = 6. $^{\#}p < 0.05$ and $^{\#\#}p < 0.01$ *vs.* Normal group; $^{*}p < 0.05$ and $^{**}p < 0.01$ *vs.* AOM/DSS group.

Figure 3. Effect of arctigenin on NLRP3 inflammasome activation in macrophages. (A) THP-1 cells were treated with arctigenin (0.3, 1, 3, 10, 30, or 100 μM) for 24 h. Cell viability was detected by MTT assay. (B) The THP-1 cells were treated with arctigenin (0.3, 1, 3, 10, or 30 μM) for 24 h. The proportions of apoptotic cells were detected by using Annexin V-FITC/PI assay and FACS analysis. (C, D) The THP-1 cells were primed with PMA (50 ng/mL), stimulated by LPS (2 μg/mL), then treated with or without arctigenin (3, 10, or 30 μM) for 3 h, and finally mixed with ATP (5 mM). The levels IL-1β and IL-18 in the supernatants were detected by ELISA. (E) The protein expression of pro-casapse1, caspase-1, IL-1β, and ASC in THP-1 cells was detected by western blot. (F, G) The interaction between NLRP3, ASC, and caspase-1 in THP-1 cells was measured by using immunoprecipitation and immunofluorescence analysis (Scale bars: 20 μm). (H) The mRNA expression of NLRP3 in THP-1 cells was measured by q-PCR assay. Results are expressed as the means ± S.E.M. from three independent experiments. $^{\#}p < 0.05$ and $^{\#\#}p < 0.01$ *vs.*

834 Normal group, $^{*}p < 0.05$ and $^{**}p < 0.01$ *vs.* LPS/ATP-treated group.

835

836 **Figure 4. Effect of arctigenin on the metabolism of macrophages during NLRP3**
837 **inflammasome assembly.** THP-1 cells were primed with PMA (50 ng/mL),
838 stimulated with LPS (2 μg/mL), treated with or without arctigenin (3, 10, or 30 μM)
839 for 3 h, and then mixed with ATP (5 mM). The metabolites of the cells were extracted
840 with extraction solvent (methanol: acetonitrile: water= 2:2:1 v/v/v). The extract was
841 taken for the UHPLC-QTOF-MS analysis using a UHPLC system (1290, Agilent
842 Technologies) with a UPLC BEH Amide column (1.7 μm 2.1*100 mm, Waters)
843 coupled to TripleTOF 6600 (Q-TOF, AB Sciex). (A) The representative total ion
844 current (TIC) chromatogram of serum samples in the ESI positive ion mode and
845 negative ion mode. (B) The PCA plots of cell samples obtained from the normal
846 group, model group, and arctigenin (10 μM) group. (C) S-plots generated from the
847 OPLS-DA model between the normal group and model group in the ESI positive ion
848 mode and negative ion mode. (D) Heatmap based on the relative abundance of 25
849 metabolites. (E) The Venn plot of metabolites in the normal group, model group, and
850 arctigenin group. The value in the middle represents the number of the metabolites
851 changed in the 3 groups. (F) Pathway analysis between the normal group and the
852 model group, and the model group and the arctigenin group. Each shape indicates one
853 metabolic pathway. The color and size of the shapes represent the effects of arctigenin
854 on metabolism, relative to the model group. The abundance of metabolites was
855 analyzed by Student's t-test ($P < 0.05$) based on the variable importance in the
856 projection in an orthogonal partial least square discriminant analysis. The Y-axis is the
857 value of negative ln(P) from pathway enrichment analysis. The X-axis is the value of
858 impact corresponding to a differentially expressed metabolite to the total metabolites
859 on a pathway. Normal: normal control group; Model: LPS /ATP-treated group;
860 Arctigenin: arctigenin (10 μM)-treated group.

Figure 5. Effect of arctigenin on FAO during NLRP3 inflammasome assembly in macrophages. THP-1 cells were primed with PMA (50 ng/mL), stimulated with LPS (2 μg/mL), treated with or without arctigenin (3, 10, 30 μM) for 3 h, and then mixed with ATP (5 mM). (A) The acetyl-coenzyme A level in the THP-1 cells was detected using an acetyl-coenzyme A assay kit. (B, C) OCR and ECAR of THP-1 cells were monitored by Seahorse XFe96 analyzer. (D) The activity of CPT1 in THP-1 cells was detected by colorimetry. (E, F) The mRNA and protein expressions of CPT1 in THP-1 cells were detected by q-PCR and western blotting, respectively. Results are expressed as the means ± S.E.M. from three independent experiments. $^{\#}p < 0.05$ and $^{\#\#}p < 0.01$ *vs.* Normal group, $^{*}p < 0.05$ and $^{**}p < 0.01$ *vs.* LPS/ATP-treated group.

Figure 6. Effect of CPT1 overexpression on the disruption of NLRP3 inflammasome assembly by arctigenin in macrophages. THP-1 cells were primed with PMA (50 ng/mL), and transfected with CPT1 plasmid or normal control plasmid, followed by incubation with LPS (2 μg/mL) for 3 h. The cells were then treated with or without arctigenin (10 μM) for 3 h, and finally mixed with ATP (5 mM). (A) THP-1 cells were transfected with CPT1 plasmid or blank control vector, and the mRNA expression of CPT1 in THP-1 cells was detected by using q-PCR. (B) The level of acetyl-coenzyme A in the THP-1 cells was detected using an acetyl-coenzyme A assay kit. (C) ASC oligomerization in THP-1 cells was detected by immunofluorescence (Scale bars: 20 μm). (D) IL-1β expression in the cell lysates was detected by ELISA. (E) The protein expressions of cleaved caspase-1 and IL-1β were detected by western blot. Results are expressed as the means ± S.E.M. from three independent experiments. $^{\#\#}p < 0.01$ *vs.* Normal group, $^{*}p < 0.05$ and $^{**}p < 0.01$ *vs.* LPS/ATP-treated group. $^{\$\$}p < 0.01$ *vs.* arctigenin (10 μM)-treated group.

887

888 **Figure 7. Effect of arctigenin on α-tubulin acetylation during NLRP3**
889 **inflammasome activation in macrophages**. THP-1 cells were primed with PMA (50
890 ng/mL), stimulated with LPS (2 μg/mL), treated with or without arctigenin (3, 10, 30
891 μM) for 3 h, and then mixed with ATP (5 mM). (A) The protein expressions of
892 α-tubulin and acetylated α-tubulin in THP-1 cells were detected by western blot. (B)
893 THP-1 cells were primed with PMA (50 ng/mL) and transfected with CPT1 plasmid
894 or normal control plasmid, followed by incubation with LPS (2 μg/mL) for 3 h. The
895 cells were then treated with or without arctigenin (3, 10, or 30 μM) for 3 h, and finally
896 mixed with ATP (5 mM). The effect of CPT1 overexpression on the inhibition of
897 α-tubulin acetylation by arctigenin in THP-1 cells was examined. (C) The interaction
898 between acetylated α-tubulin and ASC in THP-1 cells was evaluated by
899 immunofluorescence analyses (Scale bars: 20 μm). Results are expressed as the
900 means ± S.E.M. from three independent experiments. $^{\#\#}p < 0.01$ *vs.* Normal group, $^{*}p$
901 < 0.05 and $^{**}p < 0.01$ *vs.* LPS/ATP-treated group. $^{\$\$}p < 0.01$ *vs.* arctigenin (10 μM)
902 -treated group.

903

904 **Figure 8. Effect of CPT1 overexpression on the inhibitory effect of arctigenin on**
905 **CAC and inflammasome activation in the colons of mice.** (A) Percent survival rate
906 (d, days) (B) Percent weight change. (C) The length of the mouse colons. (D) The
907 number of tumors in the mouse colon tissues. (E) The size of the tumors in the mouse
908 colon tissues. (F) The tumor load in the mouse colon tissues. (G) The histological
909 changes of the colons were detected using hematoxylin-eosin staining (Scale bar: 50
910 μm) (H) Infiltration by $CD68^{+}$ $NLRP3^{+}$ cells was evaluated by immunofluorescence
911 histochemistry (Scale bars: 100 μm). (I) The expression of IL-1β, in the mouse colon
912 tissues was detected by ELISA. Results are expressed as the means ± S.E.M. from

three independent experiments. n=5-8. $^{\#}p < 0.05$, $^{\#\#}p < 0.01$ *vs.* Normal group; $^{*}p < 0.05$, $^{**}p < 0.01$ *vs.* AOM/DSS group. $^{\$\$}p < 0.01$ *vs.* arctigenin (25 mg/kg) group.

Figure 9. Correlation of CPT1 expression with CAC severity and IL-1β level in colon tissues of mice treated with arctigenin. (A) Correlation between CPT1 expression and tumor number. (B) Correlation between CPT1 expression and tumor sizes. (C) Correlation between CPT1 expression and tumor load. (D) Correlation between CPT1 expression and histological scores. (E) Correlation between CPT1 expression and IL-1β level. R = Spearman's rank correlation coefficient. A *P*-value < 0.05 was considered to show a significant difference; n = 5-8.

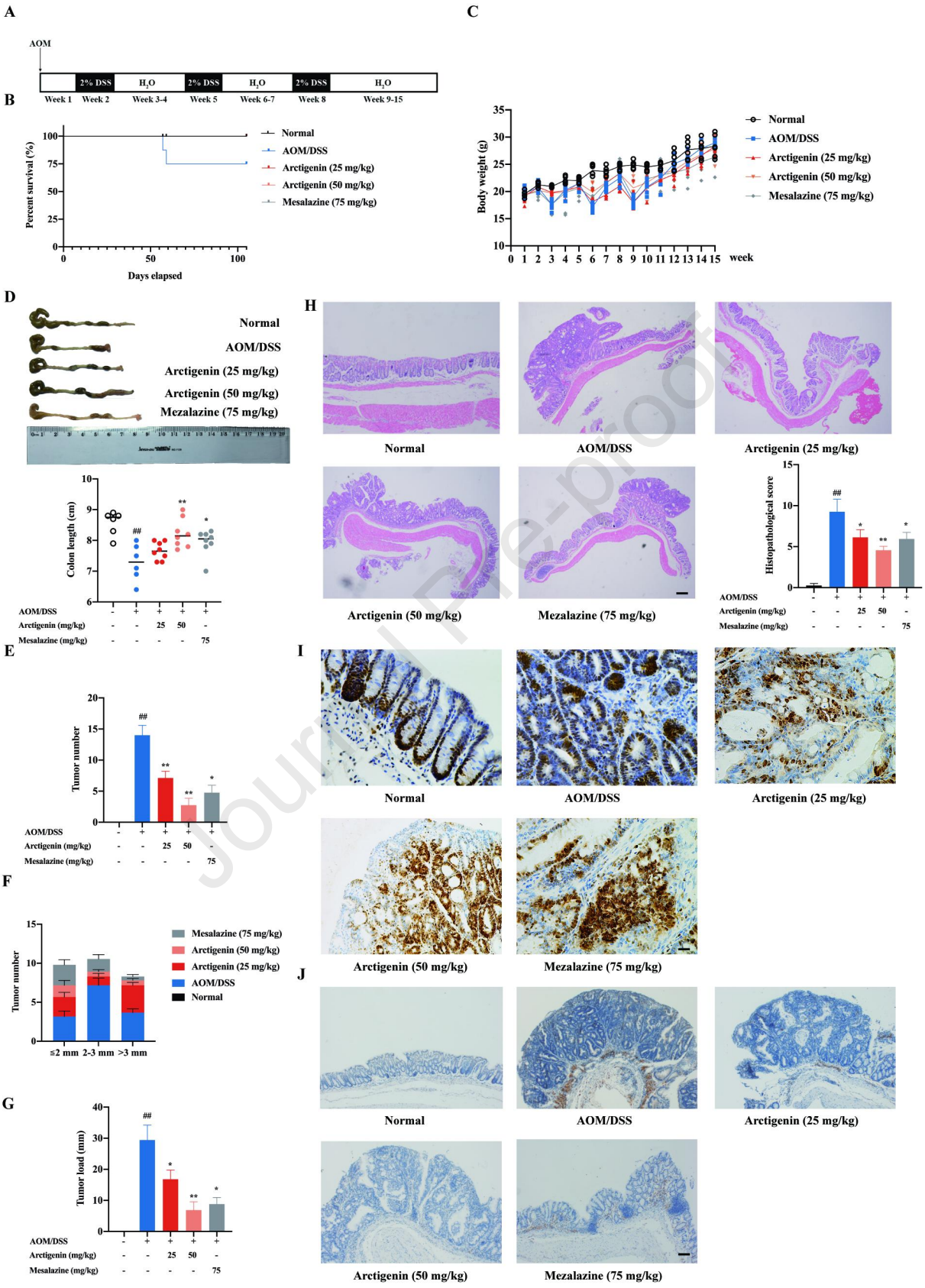

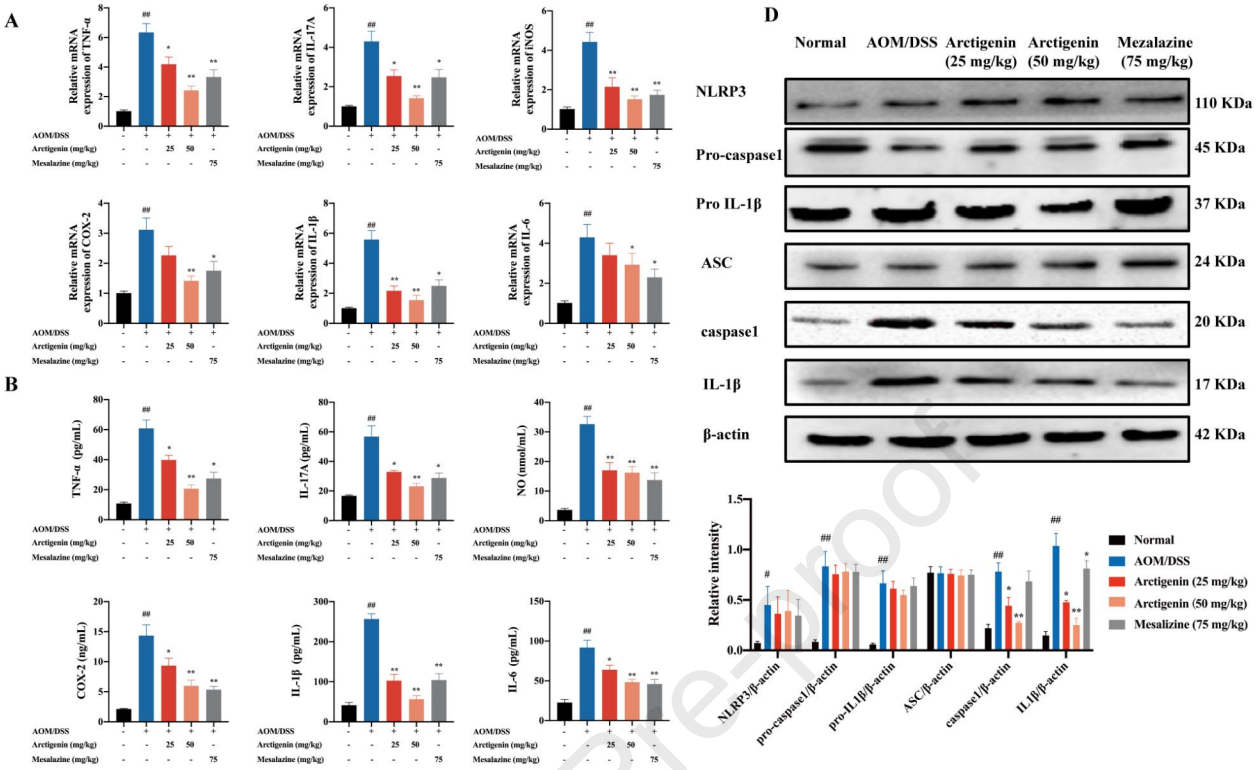
A
Relative mRNA expression of TNF-α
Relative mRNA expression of IL-17A
Relative mRNA expression of iNOS
Relative mRNA expression of COX-2
Relative mRNA expression of IL-1β
Relative mRNA expression of IL-6
AOM/DSS
Arctigenin (mg/kg)
Mesalazine (mg/kg)
B
TNF-α (pg/mL)
IL-17A (pg/mL)
NO (nmol/mL)
COX-2 (ng/mL)
IL-1β (pg/mL)
IL-6 (pg/mL)
D
Normal
AOM/DSS
Arctigenin (25 mg/kg)
Arctigenin (50 mg/kg)
Mezalazine (75 mg/kg)
NLRP3
Pro-caspase1
Pro IL-1β
ASC
caspase1
IL-1β
β-actin
110 KDa
45 KDa
37 KDa
24 KDa
20 KDa
17 KDa
42 KDa
Relative intensity
NLRP3/β-actin
pro-caspase1/β-actin
pro-IL1β/β-actin
ASC/β-actin
caspase1/β-actin
IL1β/β-actin

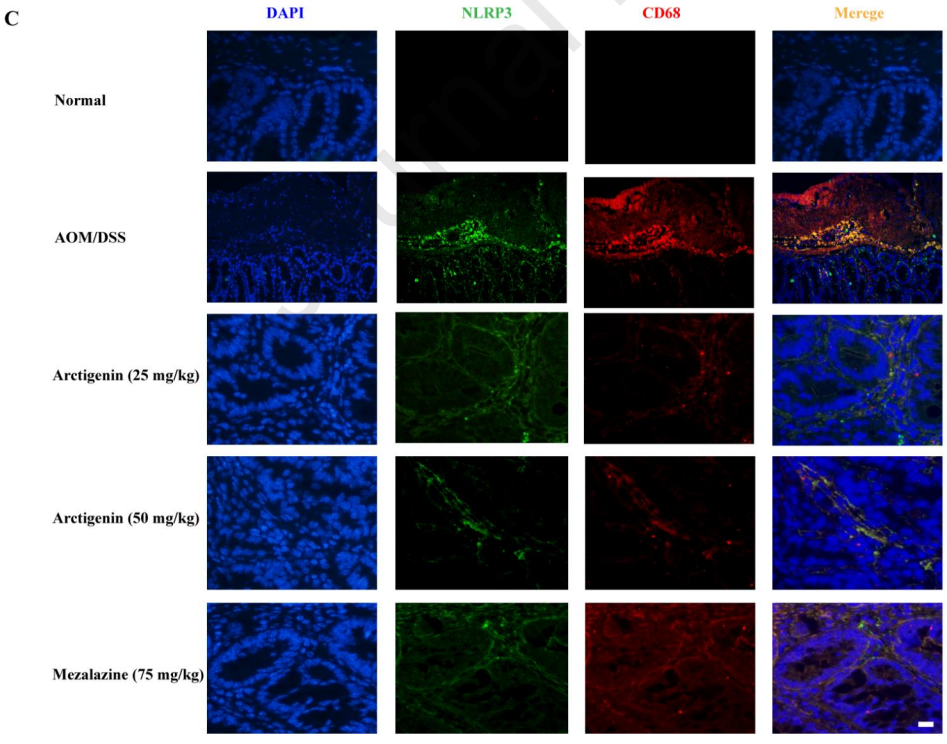
C
DAPI
NLRP3
CD68
Merege
Normal
AOM/DSS
Arctigenin (25 mg/kg)
Arctigenin (50 mg/kg)
Mezalazine (75 mg/kg)

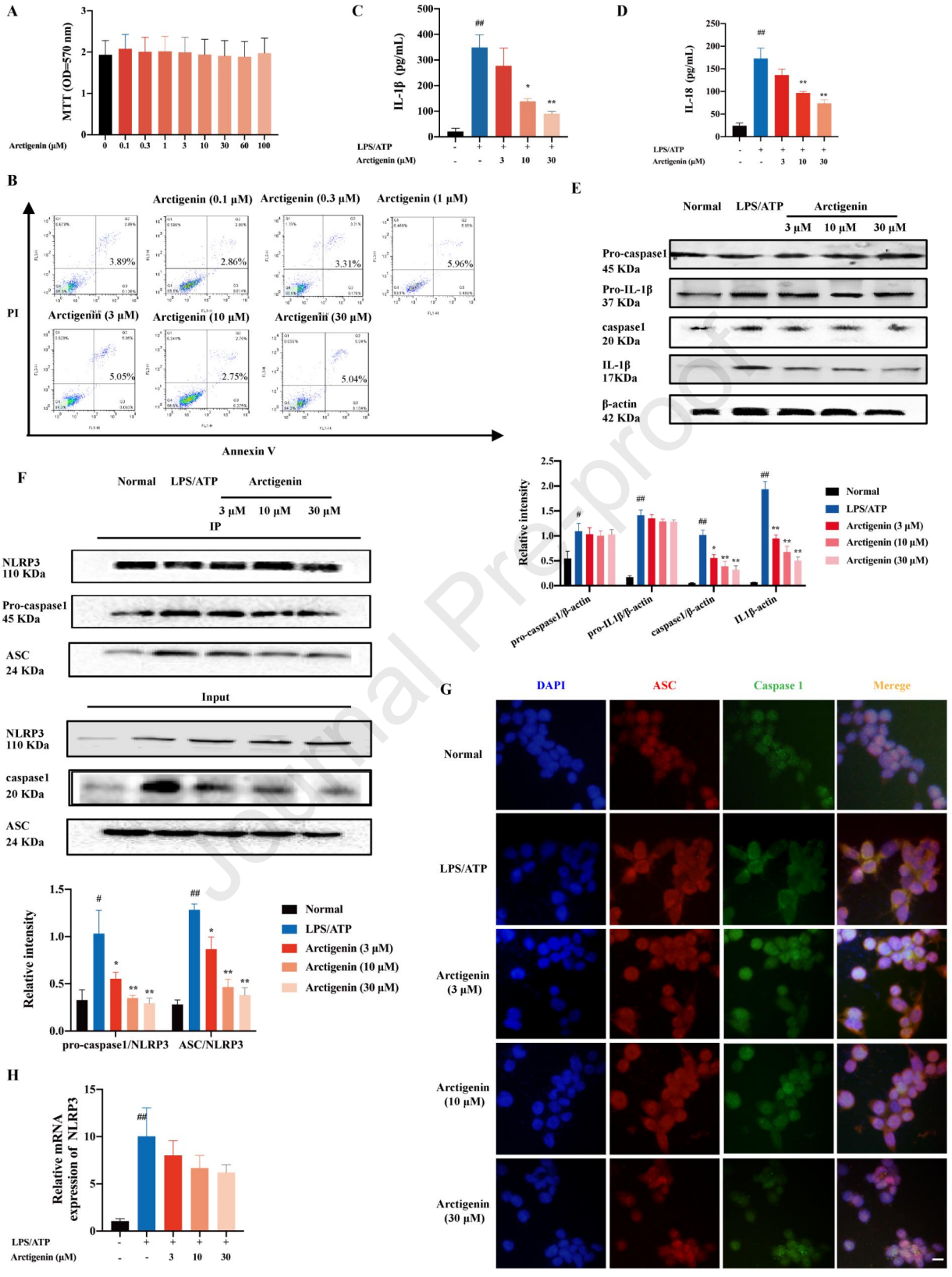

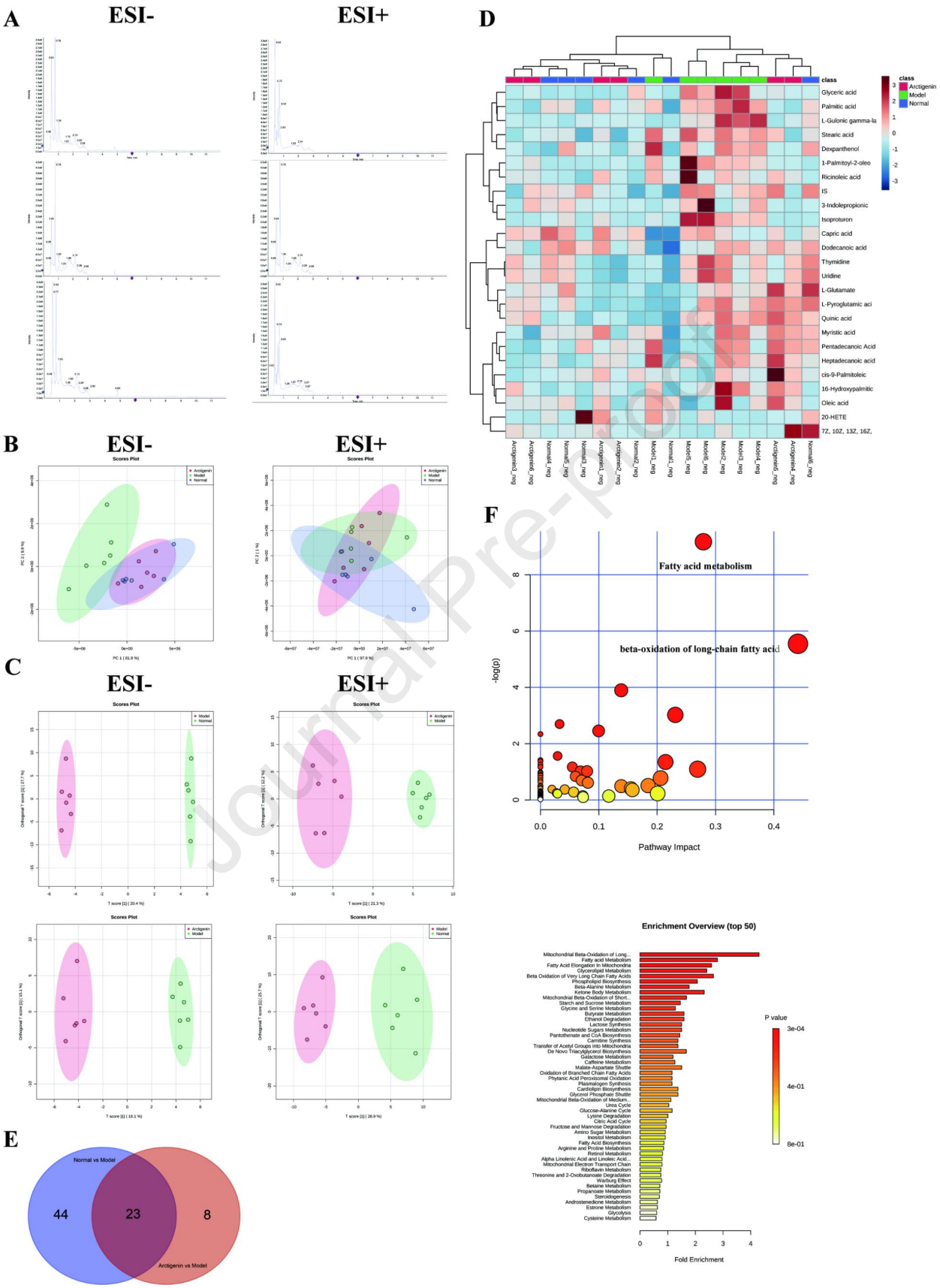

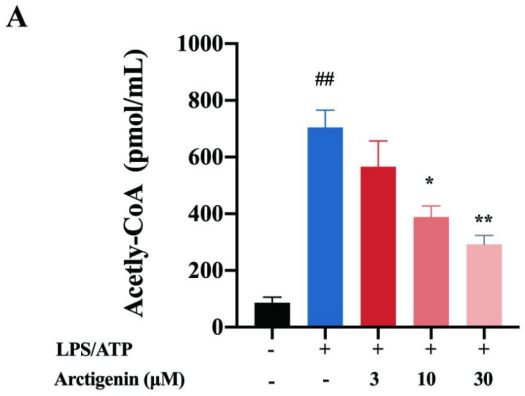

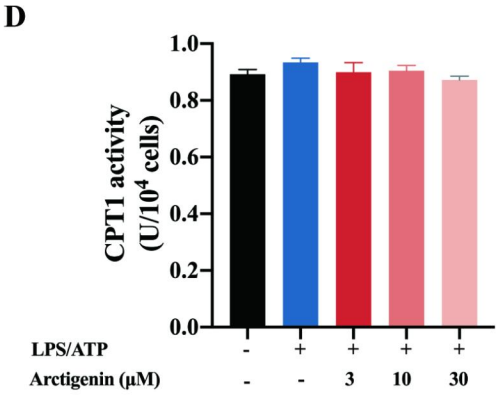

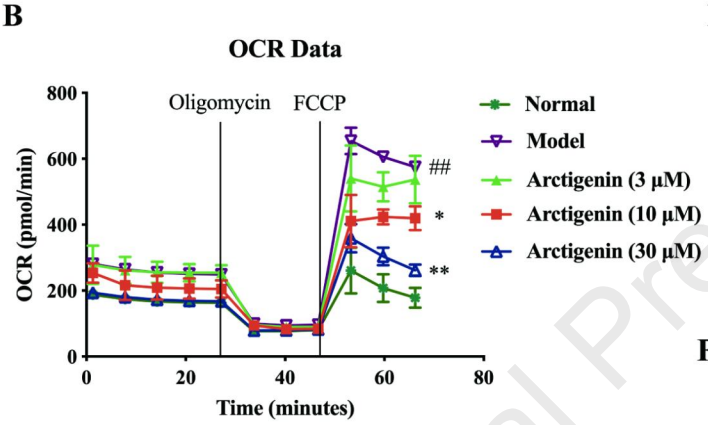

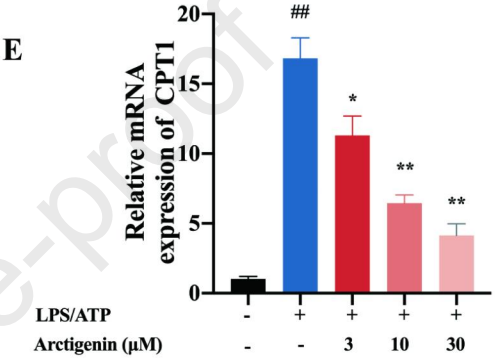

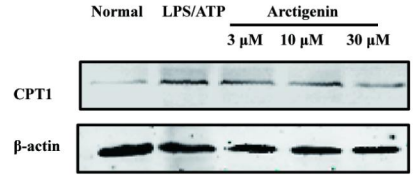

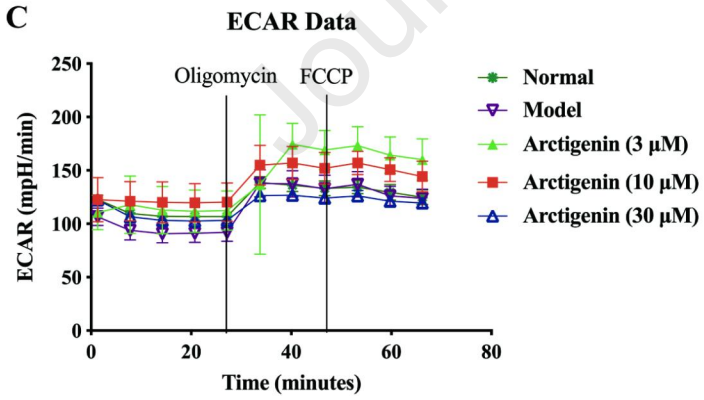

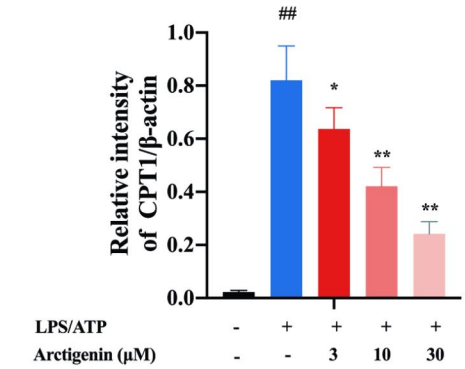

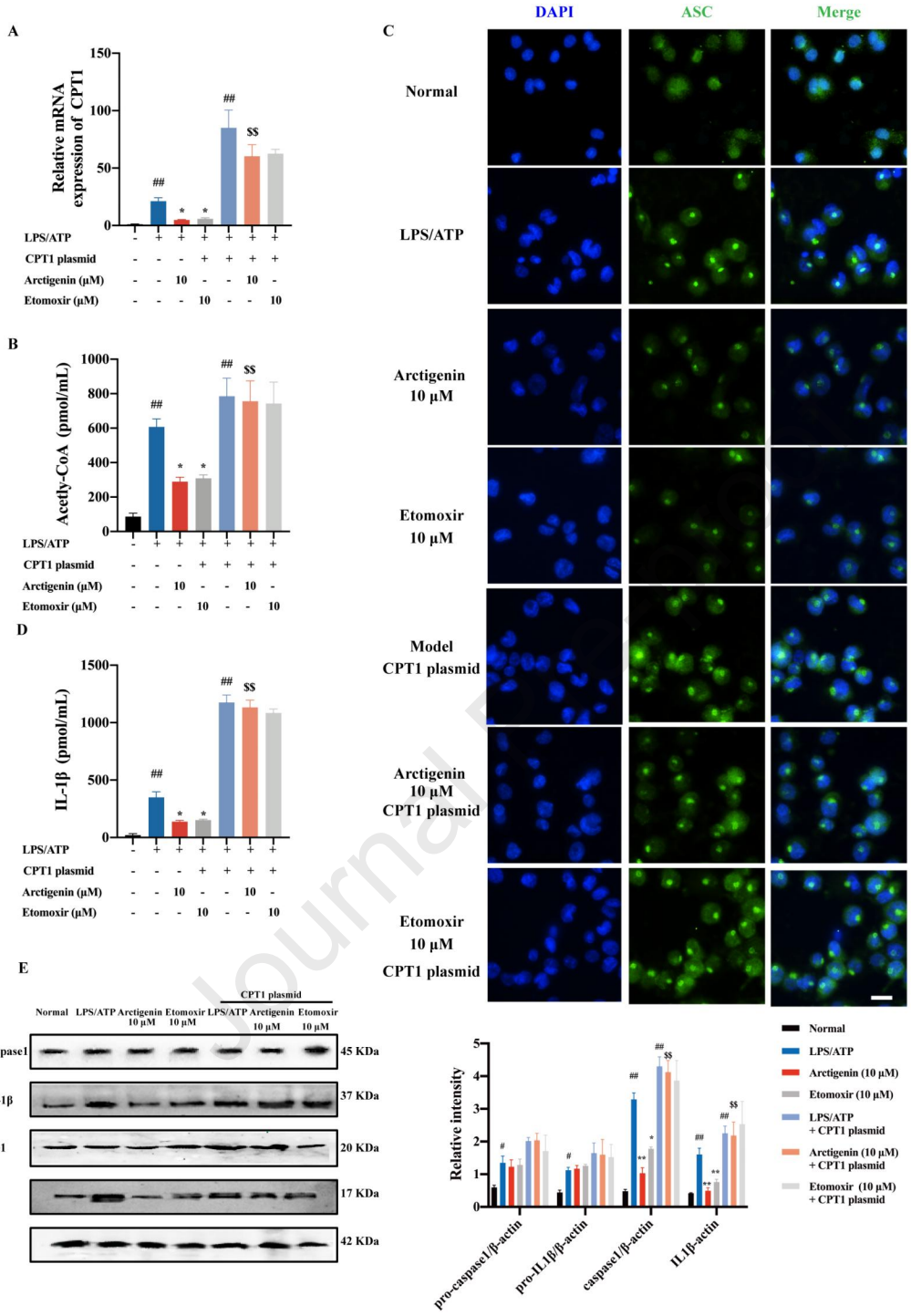
A
Relative mRNA expression of CPT1
150
100
50
0
##
*
*
##
$$
LPS/ATP - + + + + + +
CPT1 plasmid - - - + + + +
Arctigenin (μM) - - 10 - - 10 -
Etomoxir (μM) - - - 10 - - 10
B
Acetly-CoA (pmol/mL)
1000
800
600
400
200
0
##
*
*
##
$$
LPS/ATP - + + + + + +
CPT1 plasmid - - - + + + +
Arctigenin (μM) - - 10 - - 10 -
Etomoxir (μM) - - - 10 - - 10
D
IL-1β (pmol/mL)
1500
1000
500
0
##
*
*
##
$$
LPS/ATP - + + + + + +
CPT1 plasmid - - - + + + +
Arctigenin (μM) - - 10 - - 10 -
Etomoxir (μM) - - - 10 - - 10
E
CPT1 plasmid
Normal
LPS/ATP
Arctigenin 10 μM
Etomoxir 10 μM
LPS/ATP
Arctigenin 10 μM
Etomoxir 10 μM
Pro-caspase1
Pro-IL-1β
caspase1
IL-1β
β-actin
45 KDa
37 KDa
20 KDa
17 KDa
42 KDa
C
DAPI
ASC
Merge
Normal
LPS/ATP
Arctigenin 10 μM
Etomoxir 10 μM
Model CPT1 plasmid
Arctigenin 10 μM CPT1 plasmid
Etomoxir 10 μM CPT1 plasmid
Relative intensity
5
4
3
2
1
0
pro-caspase1/β-actin
pro-IL1β/β-actin
caspase1/β-actin
IL1β-actin
Normal
LPS/ATP
Arctigenin (10 μM)
Etomoxir (10 μM)
LPS/ATP + CPT1 plasmid
Arctigenin (10 μM) + CPT1 plasmid
Etomoxir (10 μM) + CPT1 plasmid

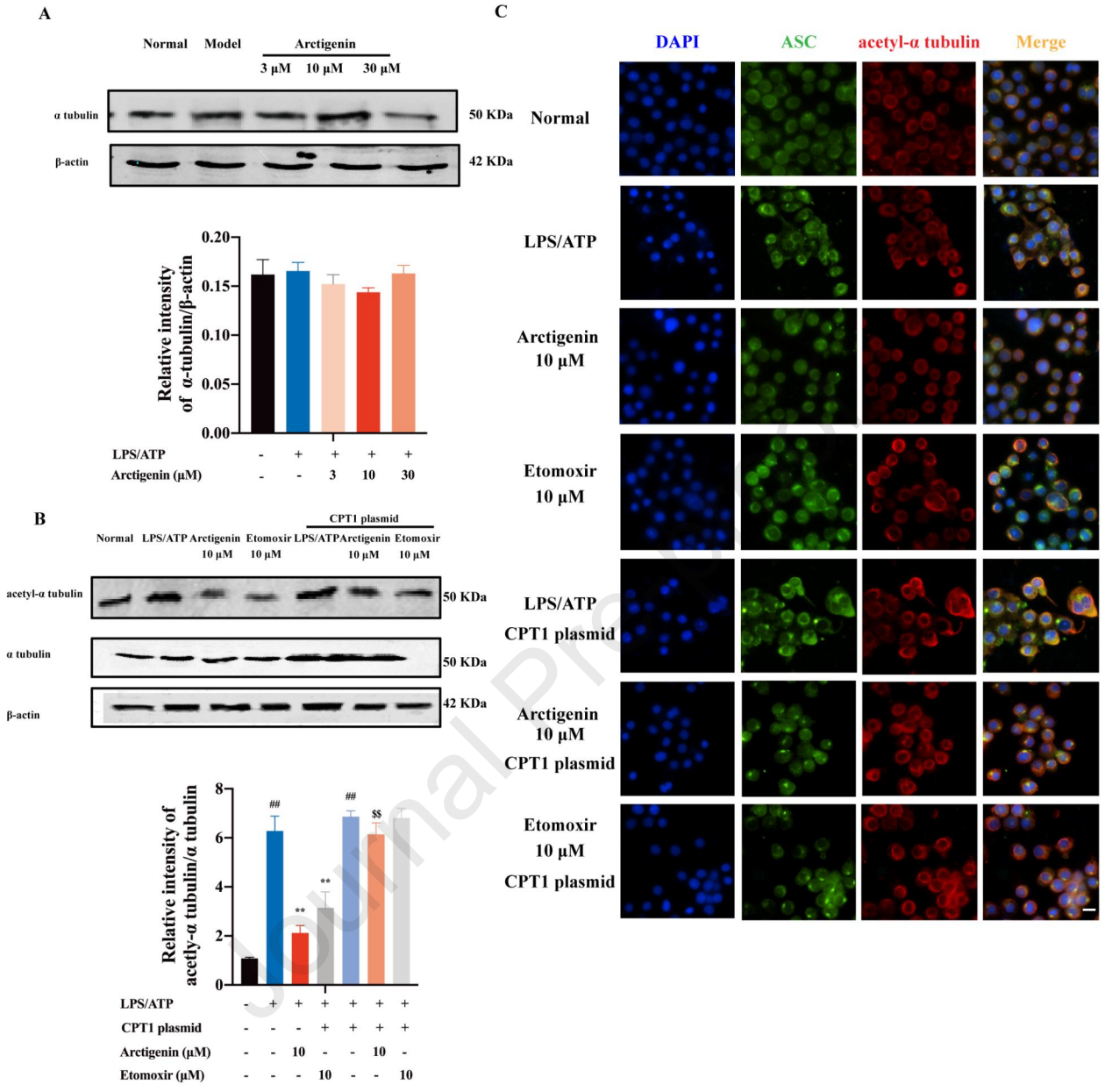
A
Normal
Model
Arctigenin
3 μM
10 μM
30 μM
α tubulin
β-actin
50 KDa
42 KDa
Relative intensity of α-tubulin/β-actin
0.20
0.15
0.10
0.05
0.00
LPS/ATP - + + + +
Arctigenin (μM) - - 3 10 30
B
CPT1 plasmid
Normal
LPS/ATP
Arctigenin 10 μM
Etomoxir 10 μM
LPS/ATP
Arctigenin 10 μM
Etomoxir 10 μM
acetyl-α tubulin
α tubulin
β-actin
50 KDa
50 KDa
42 KDa
Relative intensity of acetly-α tubulin/α tubulin
8
6
4
2
0
##
**
**
##
$$
LPS/ATP - + + + + + +
CPT1 plasmid - - - + + + +
Arctigenin (μM) - - 10 - - 10 -
Etomoxir (μM) - - - 10 - - 10
C
DAPI
ASC
acetyl-α tubulin
Merge
Normal
LPS/ATP
Arctigenin 10 μM
Etomoxir 10 μM
LPS/ATP CPT1 plasmid
Arctigenin 10 μM CPT1 plasmid
Etomoxir 10 μM CPT1 plasmid

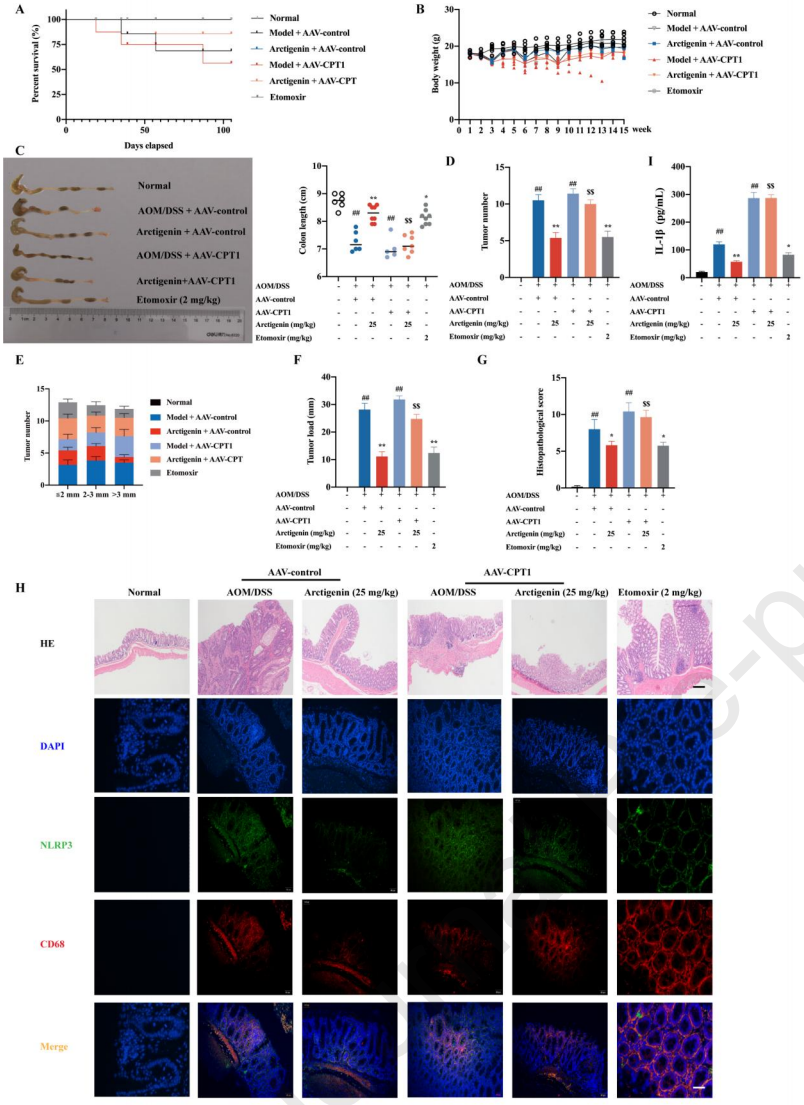
A
Percent survival (%)
Days elapsed
Normal
Model + AAV-control
Arctigenin + AAV-control
Model + AAV-CPT1
Arctigenin + AAV-CPT
Etomoxir
B
Body weight (g)
week
Normal
Model + AAV-control
Arctigenin + AAV-control
Model + AAV-CPT1
Arctigenin + AAV-CPT1
Etomoxir
C
Normal
AOM/DSS + AAV-control
Arctigenin + AAV-control
AOM/DSS + AAV-CPT1
Arctigenin+AAV-CPT1
Etomoxir (2 mg/kg)
Colon length (cm)
D
Tumor number
I
IL-1β (pg/mL)
AOM/DSS
AAV-control
AAV-CPT1
Arctigenin (mg/kg)
Etomoxir (mg/kg)
E
Tumor number
≤2 mm
2-3 mm
>3 mm
F
Tumor load (mm)
G
Histopathological score
H
AAV-control
AAV-CPT1
Normal
AOM/DSS
Arctigenin (25 mg/kg)
Etomoxir (2 mg/kg)
HE
DAPI
NLRP3
CD68
Merge

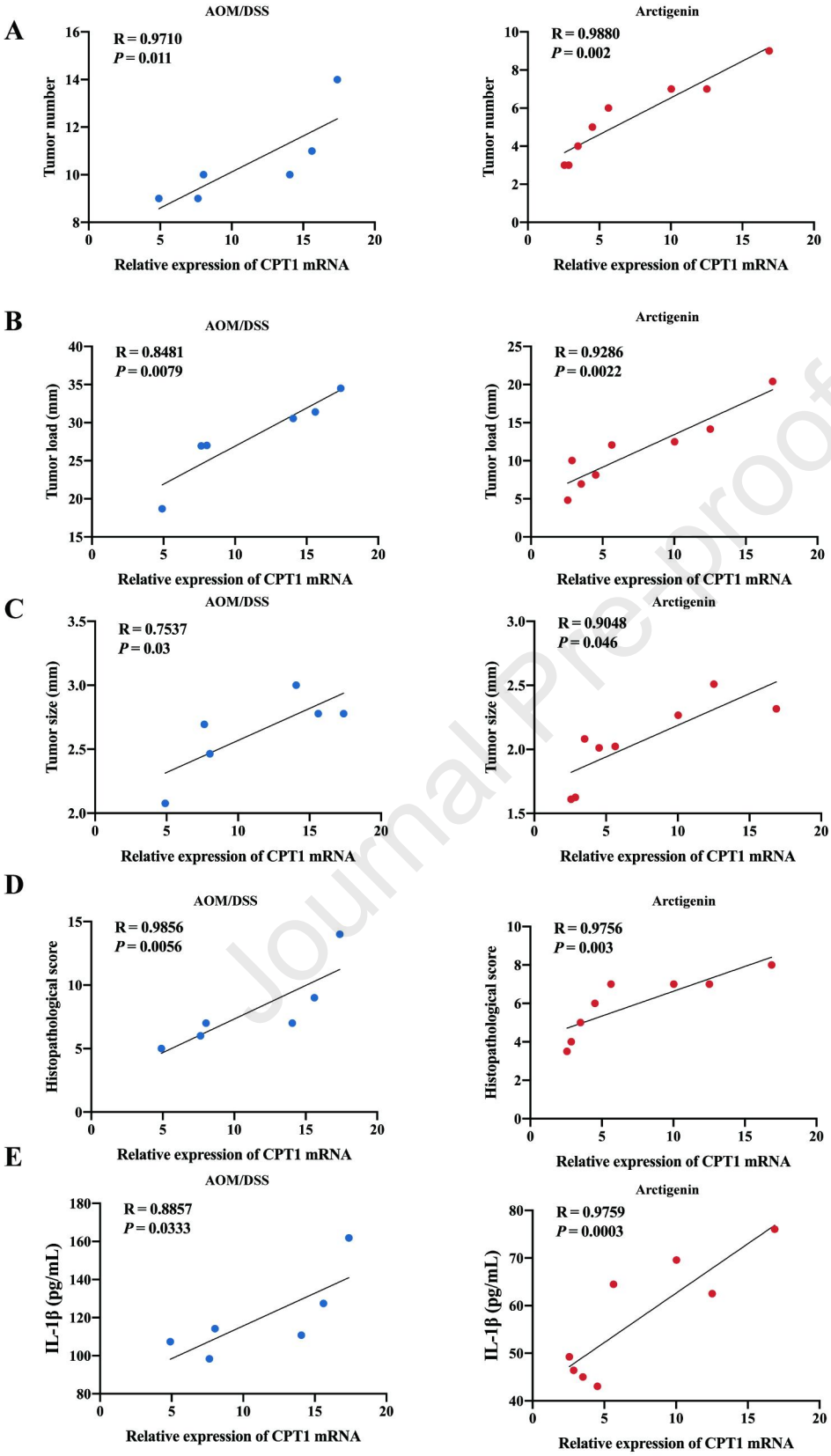

1. Oral arctigenin can effectively prevent colitis associated cancer (CAC) in mice;
2. Arctigenin selectively downregulates IL-1β expression in the colon of CAC mice;
3. Arctigenin disrupts NLRP3 inflammasome assembly to downregulate IL-1β expression;
4. Arctigenin functions by inhibiting fatty acid oxidation *via* targeting at CPT1.

Declaration of interests

☒ The authors declare that they have no known competing financial interests or personal relationships that could have appeared to influence the work reported in this paper.

☐The authors declare the following financial interests/personal relationships which may be considered as potential competing interests: